

LIBRARY
Michigan State
University

This is to certify that the
thesis entitled

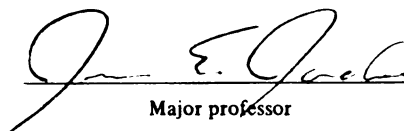
**Syntheses, Structures, and Magnetic Properties of
Lanthanide Complexes of 2,2',2''-Nitrilotriphenolates**

presented by

Lars Peereboom

has been accepted towards fulfillment
of the requirements for

M.S. degree in Chemistry


Major professor

Date 8 August 2001

PLACE IN RETURN BOX to remove this checkout from your record.
TO AVOID FINES return on or before date due.
MAY BE RECALLED with earlier due date if requested.

DATE DUE	DATE DUE	DATE DUE

**SYNTHESES, STRUCTURES, AND MAGNETIC PROPERTIES OF
LANTHANIDE COMPLEXES OF 2,2',2''-NITRILOTRIPHENOLATES**

By

Lars Peereboom

A THESIS

**Submitted to
Michigan State University
in partial fulfillment of the requirements
for the degree**

MASTER OF SCIENCE

Department of Chemistry

2001

ABSTRACT

SYNTHESES, STRUCTURES, AND MAGNETIC PROPERTIES OF LANTHANIDE COMPLEXES OF 2,2',2''-NITRILOTRIPHENOLATES

By

Lars Peereboom

Tripod ligand 2,2',2''-nitrilotriphenol (triol) can readily be deprotonated to form a trianionic ligand which reacts with lanthanide (Ln) chlorides; variation of this reaction's stoichiometry allows assembly of 1:1 and 2:1 ligand:lanthanide complexes. X-ray crystallography finds that La and Gd 1:1 complexes form phenoxide bridged dimers with Ln-Ln distances of 3.9745(3) and 3.8719(8), respectively. Gd and Yb 2:1 compounds form trianionic "sandwich" cores with two ligands capping the lanthanide; bridging sodium ions then link these complexes into parallel chains. Magnetic studies show the Gd 1:1 complex to have antiferromagnetic Gd-Gd coupling ($J = -0.058$, assuming $g=2.0$) in the normal range for systems with similar Gd-Gd distances. Three related ligands, tris(2-hydroxy-5-nitrophenyl)amine, tris(5-bromo-2-hydroxyphenyl)amine, and tris(4,5-dibromo-2-hydroxyphenyl)-amine were synthesized, and the trinitro compound's coordination chemistry with LaCl_3 explored.

To Lisa for putting up with me.

TABLE OF CONTENTS

LIST OF TABLES.....	v
LIST OF FIGURES.....	vii
INTRODUCTION	1
1.1. CONCEPTUAL OVERVIEW.....	1
1.2. LITERATURE REVIEW.....	2
1.3. PHENOXIDE COMPLEXES OF LANTHANIDES	5
RESULTS & DISCUSSION	9
2.1. SYNTHESIS OF LIGANDS.....	9
2.2. SYNTHESIS OF COMPLEXES	12
2.3. NMR ANALYSIS	13
2.4. MASS SPECTROMETRIC ANALYSIS.....	17
2.5. X-RAY STRUCTURES	18
2.6. MAGNETIC STUDIES.....	26
EXPERIMENTAL	31
3.1. EQUIPMENT AND CHEMICALS USED.....	31
3.2. SYNTHESIS:	32
3.2.1. Ligands.....	32
3.2.2. Complexes.....	37
3.3. IR	39
3.4. NMR STUDIES.....	39
3.5. SQUID MEASUREMENTS.....	40
3.6. X-RAY CRYSTALLOGRAPHY	41
APPENDIX.....	44
LIST OF REFERENCES.....	74

LIST OF TABLES

Table

2.1	Bonds and angles of lanthanide triolate complexes.....	18
2.2	Magnetic coupling constants for gadolinium dimer complexes.	29
A.1	Crystallographic data for $\text{La}_2(\text{triolate})_2 \cdot 6\text{DMSO}$ 28	53
A.2	Crystallographic data for $\text{Gd}_2(\text{triolate})_2 \cdot 4\text{DMSO}$ 29	54
A.3	Crystallographic data for $\text{Na}_3\text{Gd}(\text{triolate})_2 \cdot 2\text{H}_2\text{O} \cdot 6\text{CH}_3\text{OH}$ 32	55
A.4	Crystallographic data for $\text{Na}_3\text{Yb}(\text{triolate})_2 \cdot 2\text{H}_2\text{O} \cdot 5\text{CH}_3\text{OH}$ 33 ...	56
A.5	Atomic coordinates ($\times 10^4$), equivalent isotropic displacement parameters ($\text{\AA}^2 \times 10^3$), and occupancies for $\text{La}_2(\text{triolate})_2 \cdot 6\text{DMSO}$ 28	57
A.6	Anisotropic displacement parameters ($\text{\AA}^2 \times 10^3$) for $\text{La}_2(\text{triolate})_2 \cdot 6\text{DMSO}$ 28	61
A.7	Atomic coordinates ($\times 10^4$), equivalent isotropic displacement parameters ($\text{\AA}^2 \times 10^3$), and occupancies for $\text{Gd}_2(\text{triolate})_2 \cdot 4\text{DMSO}$ 29	63
A.8	Anisotropic displacement parameters ($\text{\AA}^2 \times 10^3$) for $\text{Gd}_2(\text{triolate})_2 \cdot 4\text{DMSO}$ 29	65
A.9	Atomic coordinates ($\times 10^4$), equivalent isotropic displacement parameters ($\text{\AA}^2 \times 10^3$), and occupancies for $\text{Na}_3\text{Gd}(\text{triolate})_2 \cdot 2\text{H}_2\text{O} \cdot 6\text{CH}_3\text{OH}$ 32	66
A.10	Anisotropic displacement parameters ($\text{\AA}^2 \times 10^3$) for $\text{Na}_3\text{Gd}(\text{triolate})_2 \cdot 2\text{H}_2\text{O} \cdot 6\text{CH}_3\text{OH}$ 32	68

A.11	Atomic coordinates ($\times 10^4$), equivalent isotropic displacement parameters ($\text{\AA}^2 \times 10^3$), and occupancies for $\text{Na}_3\text{Yb}(\text{triolate})_2 \cdot 2\text{H}_2\text{O} \cdot 5\text{CH}_3\text{OH}$ 33	69
A.12	Anisotropic displacement parameters ($\text{\AA}^2 \times 10^3$) for $\text{Na}_3\text{Yb}(\text{triolate})_2 \cdot 2\text{H}_2\text{O} \cdot 5\text{CH}_3\text{OH}$ 33	72

TABLES OF FIGURES

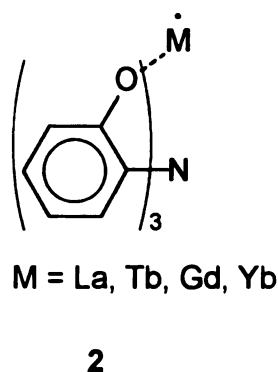
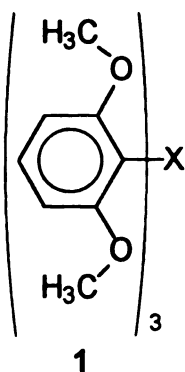
Figure		
1.1	General cage structures of atranes and aratranes. Naming follows the simple form of naming X followed by "atrane" or "aratrane" (i.e. Xatrane). Thus when X=B, the structures would be boratrane and boraratrane.....	2
1.2	Known compounds derived from tris(2-hydroxyphenyl) amine...	3
1.3	Aluminum triolate dimer 6a , showing the phenoxides bridging the two aluminum ions.....	4
2.1	¹ H-NMR spectra of Na ₃ triolate 27 , Na ₃ La(triolate) ₂ 31 , and Na ₃ Yb(triolate) ₂ 33 in D ₂ O	15
2.2	¹ H-NMR spectra of Na ₃ triolate 27 titrated with LaCl ₃ in D ₂ O....	16
2.3	ORTEP drawings of (LaTriolate) ₂ •6DMSO 28 and (GdTriolate) ₂ •4DMSO 29	20
2.4	Core structure of Na ₃ Gd(triolate) ₂ •2H ₂ O•6CH ₃ OH 32 clearly showing the diaratrane cage.....	22
2.5	View perpendicular to the metal-containing planes of Na ₃ Gd(triolate) ₂ •2H ₂ O•6CH ₃ OH 32 and Na ₃ Yb(triolate) ₂ •2H ₂ O•5CH ₃ OH 33 ; carbon and hydrogen atoms omitted for clarity.....	24
2.6	End on view of Na ₃ Gd(triolate) ₂ •2H ₂ O•6CH ₃ OH 32 and Na ₃ Yb(triolate) ₂ •2H ₂ O•5CH ₃ OH 33 ; carbon and hydrogen atoms omitted for clarity.....	25
2.7	χT vs T curves for (●)Gd ₂ (triolate) ₂ •4DMSO 29 ; (□)Na ₃ Gd(triolate) ₂ •2H ₂ O•6CH ₃ OH 32 ; (+)Yb ₂ (triolate) ₂ •4DMSO 30 ; (x) Na ₃ Yb(triolate) ₂ •2H ₂ O•5CH ₃ OH 33 ; (—) calculated fit for Gd 1:1 29	27
A.1	FTIR spectrum of Yb ₂ (triolate) ₂ •4DMSO complex 30 (KBr pellet).....	45

A.2	FTIR spectrum of $\text{Na}_3\text{Gd}(\text{triolate})_2 \cdot 2\text{H}_2\text{O} \cdot 6\text{CH}_3\text{OH}$ 32 (KBr pellet).....	46
A.3	FTIR spectrum of $\text{Na}_3\text{La}(\text{triolate})_2 \cdot 2\text{H}_2\text{O} \cdot 6\text{CH}_3\text{OH}$ 31 (KBr pellet).....	47
A.4	FTIR spectrum of $\text{Na}_3(\text{triolate})$ 27 (KBr pellet).....	48
A.5	Drawing of $\text{La}_2(\text{triolate})_2 \cdot 6\text{DMSO}$ 28 showing thermal ellipsoids and atom labeling scheme. Hydrogens are omitted.....	49
A.6	Drawing of $\text{Gd}_2(\text{triolate})_2 \cdot 4\text{DMSO}$ 29 showing thermal ellipsoids and atom labeling scheme. Hydrogens are omitted.....	50
A.7	Drawing of $\text{Na}_3\text{Gd}(\text{triolate})_2 \cdot 2\text{H}_2\text{O} \cdot 6\text{CH}_3\text{OH}$ 32 showing thermal ellipsoids and atom labeling scheme. Hydrogens are omitted.....	51
A.8	Drawing of $\text{Na}_3\text{Yb}(\text{triolate})_2 \cdot 2\text{H}_2\text{O} \cdot 5\text{CH}_3\text{OH}$ 33 showing thermal ellipsoids and atom labeling scheme. Hydrogens are omitted.....	52

INTRODUCTION

1.1. Conceptual Overview

Recent work from the research labs of Dr. J. E. Jackson has focused on ionophoric triaryl X systems **1** where X may be a radical center, carbocation, amine, or borane¹. It was found that these "tripod ether" complexants can be assembled into magnetically interacting complexes using metal ions.² Besides X-ray structural characterization of the free triaryl X compounds, their ion binding behavior has been investigated using pulsed EPR, NMR, and UV-Vis techniques.³ Inverting the theme of magnetism based on ligand-centered radicals, my research has focused on the structurally related compounds **2** below in which paramagnetic metals are complexed by diamagnetic ligands. It is the synthesis of these compounds and their structural, spectroscopic, and magnetic characterization that form the body of this thesis.



Lanthanides are oxophilic and generally behave as hard ions with no orbital constraints on their bonding. Their complexation is therefore similar to that found with alkali metals,⁴ the principal class of ions whose coordination has been explored in this structural framework. The Lanthanides' unpaired electrons

are in *f* orbitals which are buried inside the filled *s* and *p* orbitals. This shielding prevents the *f* electrons from participating in directional bonding interactions. The bonds of lanthanides can thus be viewed as simple electrostatic interactions between their stable 3⁺ ions and the ligand.

1.2. Literature Review

(a) Atranes & related systems

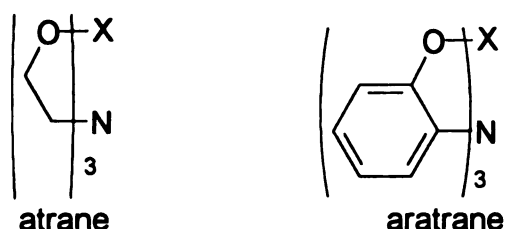
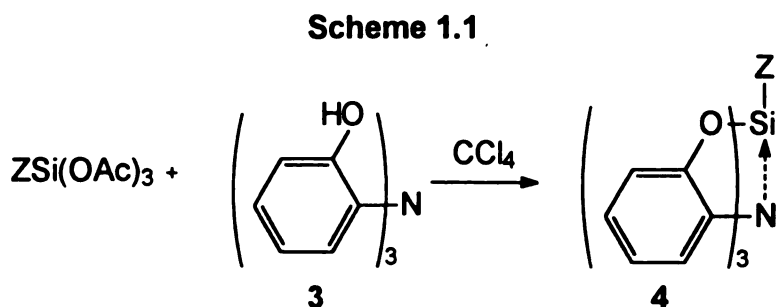


Figure 1.1: General cage structures of atranes and aratranes. Naming follows the simple form of naming X followed by “atrane” or “aratrane” (i.e. Xatrane). Thus when X=B, the structures would be boratrane and boraratrane.

In 1966 Frye et al. first reported the synthesis of 2,2',2''-nitrilotriphenol **3**.^{5,6} This ligand was prepared via the Ullmann condensation of ortho-anisidine and 2-iodoanisole followed by cleavage of the methyl ethers. Frye also used it to make pentacoordinated silicon derivatives. For example, the ligand readily reacts with phenyltriacetoxysilane to form the phenylnitrilotriphenoxysilane **4** as shown in Scheme 1.1.



Müller and Bürgi made a series of systems similar to Frye's, but incorporating boron, aluminum, and phosphorus. In X-ray diffraction studies, the free boratrane **5a** showed a bond between the boron and the central nitrogen.⁷ In later work the same authors reported X-ray structures of the boron triolate pyridine and quinuclidine adducts **5b** and **5c**.⁸ The latter compounds showed long intracage B-N distances, confirming that adduct formation destroyed the intramolecular B-N bond. Shortly thereafter, compounds **5a**, **6a**, and **7a** were also reported by Paz-Sandoval et al., characterized only by NMR and elemental analysis.⁹

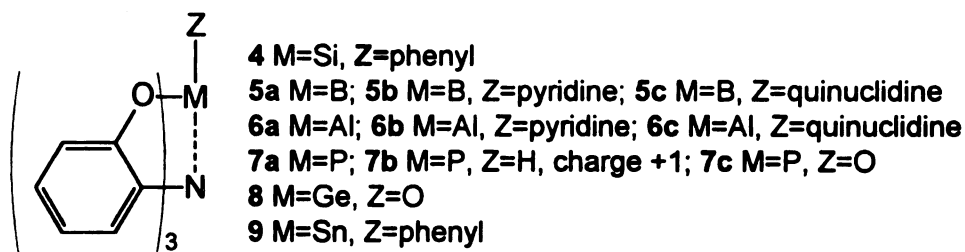


Figure 1.2: Known compounds derived from tris(2-hydroxyphenyl) amine.

The aluminum complex that Müller prepared requires an extra coordinating atom on the open faces to give 5-coordinate aluminum. Unlike the boron triolate, the aluminum triolate **6a** formed a dimer with two phenoxy oxygens bridging two aluminum centers as shown in Figure 1.3.¹⁰ The pyridine and quinuclidine adducts **6b** and **6c** were monomeric and structurally similar to those found in the boron series.

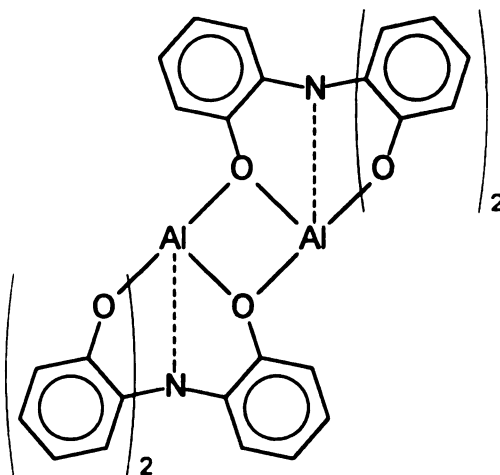
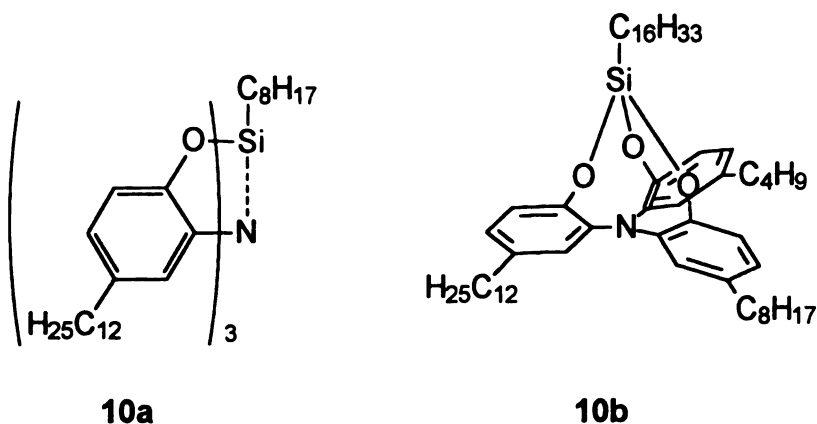


Figure 1.3: Aluminum triolate dimer **6a**, showing the phenoxide bridging the two aluminum ions.

The X-ray structure of the neutral phosphatrane **7a** showed no evidence for interaction between the P and the N. One unique chemical feature, however, is that this compound gets protonated on P, not the more electronegative N. This unusual site preference is apparently due to a strong N-P interaction in the protonated system. No structural data were given to confirm this N-P interaction,¹¹ but the analogous behavior has been thoroughly characterized in the parent aliphatic phosphatrane.¹²

Livant et al. reacted triol with germanium tetraethoxide resulting in oxygen bridged dimer **8**¹³. This dimer consist of two germa-aratranes bridged by a single oxygen atom. The phenyl 2,2',2''-nitritotriphenoxy stannane **9** was made by Ravenscroft¹⁴ for the study of mercuridestannylation of phenylstannatranes. To our knowledge this is the only reported example of a heavy-metal complex; unfortunately, the authors provided no structural information for this species.



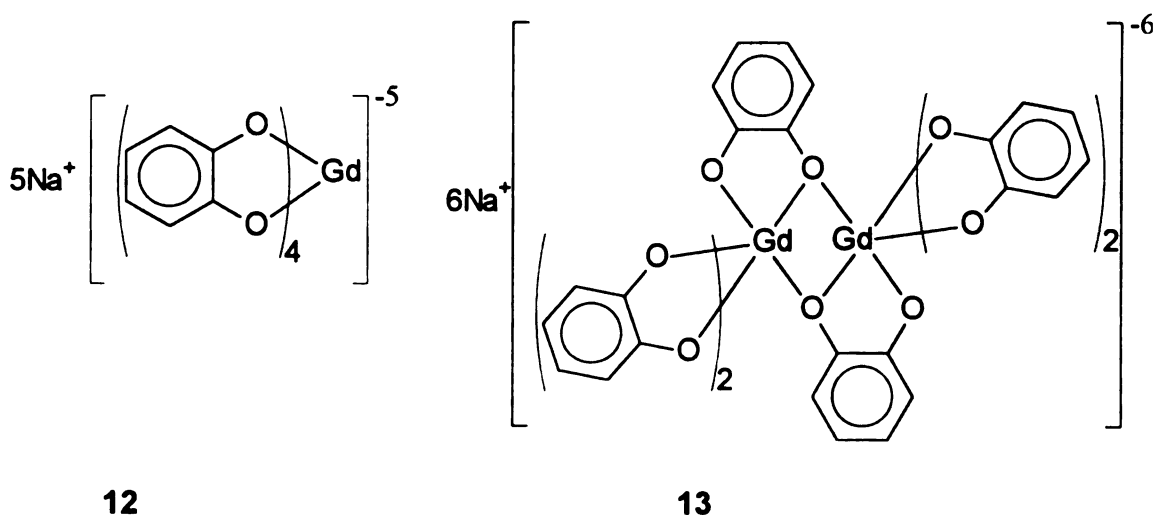
A search of the literature (CAS Online, Cambridge Structural Database, Beilstein online, and ISI) revealed only two 2,2',2''-nitritriphenol units containing additional substituents on the aryl rings. Soulie et al. prepared both the symmetrically substituted tris(2-hydroxy-5-dodecylphenyl)amine and the asymmetrically substituted (5-butyl-5'-dodecyl-5''-octyl-2,2',2''-triphenol)-amine. These two compounds were used to synthesize tetrasubstituted tribenzosilatrane **10a**¹⁵ and **10b**¹⁶. These same authors in 1993 reported the X-ray structure of tris(2-methoxyphenyl)amine **11**¹⁷ which had already been solved and reported by Müller et al. in 1989.¹⁸

1.3. Phenoxide Complexes of Lanthanides

The second body of reference literature centers on lanthanide complexes. A huge number of lanthanide alkoxides complexes are known. Many of these complexes tend to be polymeric and insoluble in most solvents. The systems most relevant to the present work are phenoxide complexes, particularly those

dimeric or oligomeric complexes that display magnetic interactions between lanthanide centers.

Two catecholate systems reported by Freeman et al.¹⁹ are of interest in that they are soluble at extremely alkaline pHs (>11). Generally, Lanthanides tend to precipitate out of solution as hydroxides at such high pH values. These particular complexes, $\text{Na}_5[\text{Gd}(\text{cat})_4] \cdot 21\text{H}_2\text{O}$ **12** and $\text{Na}_6[\text{Gd}(\text{cat})_3]_2 \cdot 20\text{H}_2\text{O}$ **13**, are polyanions in which the catecholates directly coordinate and encapsulate the lanthanide, excluding solvent molecules from the lanthanide ligand sphere. For the $\text{Na}_6[\text{Gd}(\text{cat})_3]_2 \cdot 20\text{H}_2\text{O}$ **13** species, the polyanionic dimer units are linked



through sodium and water molecules to form chains. The Gd-Gd distance in this phenoxy-bridged dimer is 3.84 Å. Unfortunately, magnetic data on these complexes were not reported.

Orvig et al.²⁰ reported interesting lanthanide N_4O_3 amine phenoxide ligand complexes that show no solvent interaction in the first lanthanide-ligand bonding sphere. The 1:1 gadolinium-(amine phenol ligand) complex **14** is a neutral,

phenoxy-bridged dimer with a Gd-Gd distance of 3.98 Å. This heptadentate lanthanide complex is stable under basic to weakly acidic conditions in both solid and solution forms.

Magnetic studies on **14** showed evidence of a weak antiferromagnetic Gd-Gd coupling ($J = -0.045 \text{ cm}^{-1}$).

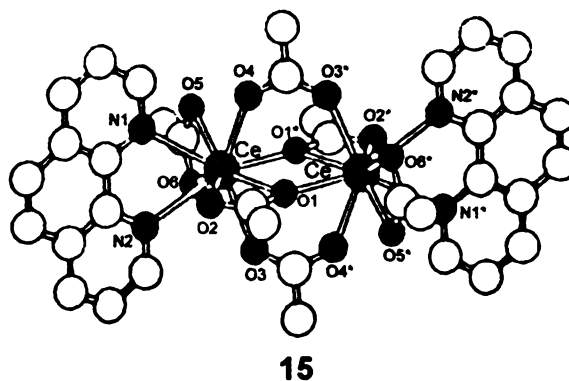
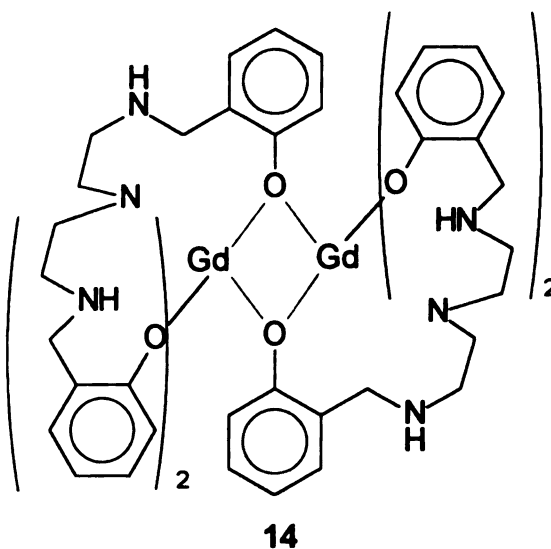
Panagiotopoulos et al.²¹,

reported two acetate-bridged

lanthanide dimers, $[\text{Ln}_2(\text{CH}_3\text{CO}_2)_6(\text{phen})_2]$ where phen is o-phenanthroline and Ln is cerium or gadolinium. Both complexes demonstrated antiferromagnetic coupling; however, only the structure

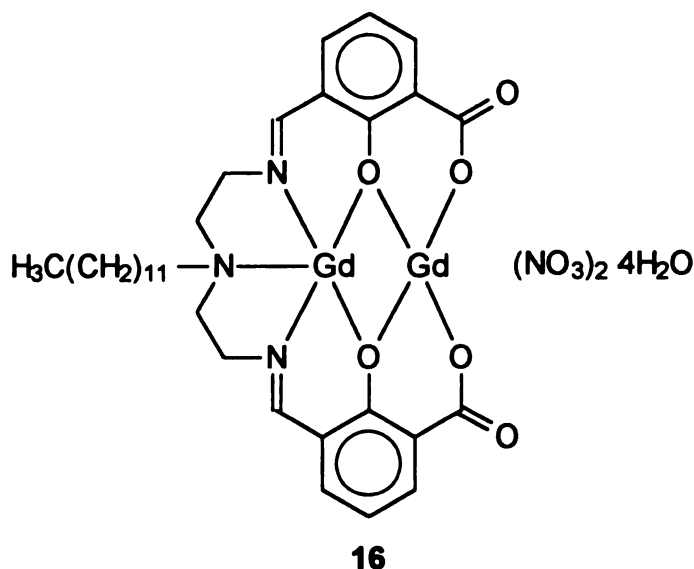
of the cerium complex **15** was reported. The cerium complex showed a Ce-Ce bond distance of 4.035 Å, and an antiferromagnetic coupling constant of $J = -0.75 \text{ cm}^{-1}$. The Gd-Gd

complex was reported to have an antiferromagnetic coupling constant of $J = -0.053 \text{ cm}^{-1}$ with the expected Gd-Gd bond distance equal to or less than that in Ce-Ce complex.



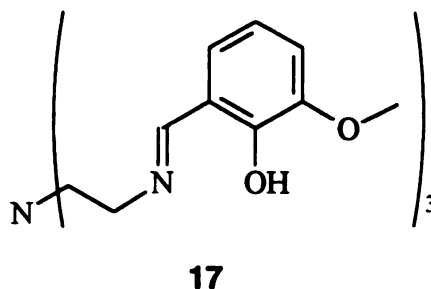
Guerriero, et al.,²² synthesized various lanthanide complexes with acyclic Schiff bases. Of particular interest is the homo-dinuclear gadolinium-Schiff base

complex **16** which shows a large antiferromagnetic coupling constant ($J = -0.24 \text{ cm}^{-1}$). The complex contains two gadolinium atoms bound in the same ligand by two phenoxy groups. Although the



structure of the complex is not known, the authors proposed that the large J value results from a superexchange phenomenon through the bridging atoms. However, the absence of large coupling constants in other phenoxide bridged complexes conflicts with this explanation.

Costes, et al., like Guerriero, synthesized lanthanide complexes with tris(4-(2-hydroxy-3-methoxyphenyl)-3-aza-3-butenyl)amine **17**.²³ They created both the Yb-La and the Gd-Gd complexes. The latter showed an antiferromagnetic interaction with a $J = -0.104 \text{ cm}^{-1}$. They did not report a structure



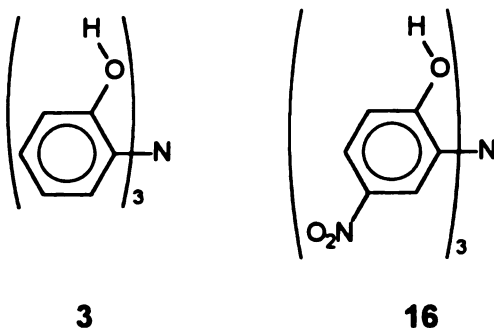
for the Gd-Gd complex but they speculated that the Gd-Gd distance should be similar to the Yb-La distance, which they reported as $3.7337(6) \text{ \AA}$.

A unique structure was synthesized by Hedinger, et al.²⁴ They reacted 1,3,5-triamino-1,3,5-trideoxy-*cis*-inositol with lanthanide salts. Their X-ray data

showed two triply deprotonated ligands encapsulating an equilateral triangle of lanthanide ions. In the gadolinium complex they measured an antiferromagnetic coupling $J = -0.092 \text{ cm}^{-1}$.

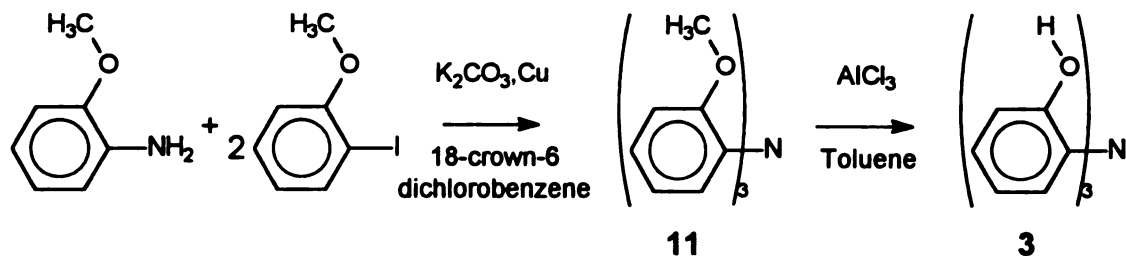
RESULTS & DISCUSSION

2.1. Synthesis of Ligands



Two ligands were synthesized and used to form complexes: triol (tris(2-hydroxyphenyl)amine) **3** and a trinitro analogue (tris(2-hydroxy-5-nitrophenyl)amine) **18**. Triol **3** was prepared according to Frye's procedure⁶ with one exception: 18-crown-6 was used as a phase transfer catalyst for the Ullman reaction²⁵ (Scheme 2.1). This alteration increased the yield to 73%. The demethylation was performed as reported by Frye and worked in good yield.

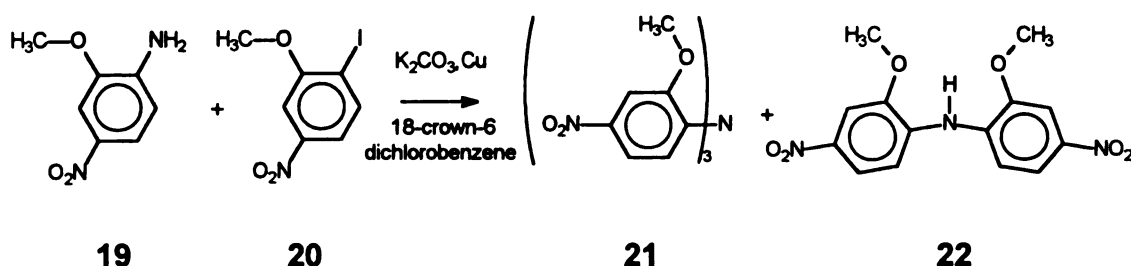
Scheme 2.1



The triolate (deprotonated triol **3**) reacts readily with oxygen. To offset this sensitivity, electron-withdrawing nitro groups were added to the aryl rings. We

attempted to make the tris(2-methoxy-4-nitrophenyl)amine **21**, by starting with 2-methoxy-4-nitroaniline **19**. This species was readily converted to 2-iodo-5-nitroanisole **20** via the diazonium salt.

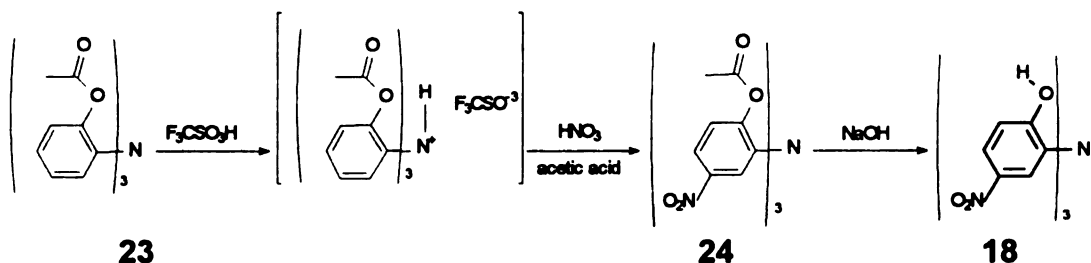
Scheme 2.2



The Ullman reaction on this system (Scheme 2.2) was not efficient. When two equivalents of 2-iodo-5-nitroanisole were used, only the diphenyl amine **22** ~35% and reduced 3-nitroanisole ~10% were obtained. With a large excess (>6 equivalents) of the iodo compound, modest yields of the desired compound **21** ~30% and diphenyl amine **22** ~30% were isolated. The remaining product was an unidentified tar-like residue. Unfortunately all attempts to demethylate the trinitro trimethoxy compound **21** with AlCl₃, BBr₃, or 40% HI failed.

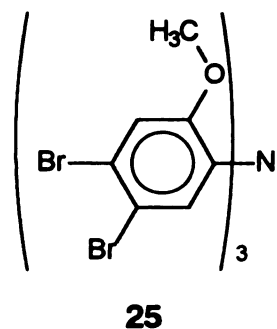
Direct nitration of trimethoxy compound **11** or triol **3** resulted in a mixture of products, each having at least one nitro group para to the central nitrogen. Some also were nitrated ortho and/or para to the hydroxy group. None of these products had three equivalent aryl rings. To prevent ortho nitration triol **3** was acetylated. This did solve the ortho nitration problem, but nitration still took place meta and para to the central nitrogen.

Scheme 2.3



To deactivate the ortho, para-directing ability of the central nitrogen, it was protonated using trifluoromethanesulfonic acid. Subsequent nitration with nitric acid in acetic acid resulted in tris(2-acetoxy-5-nitrophenyl)amine **24** (30%) and a complex mixture of other nitration products. Compound **24** is readily converted to the trinitrotriolate **18** with NaOH. Compound **18** can be converted to tris(5-amino-2-hydroxyphenyl)amine•3HCl salt **34** using Pd/C and sodium borohydride.

To make other substituted triols, attempts were made to brominate triol **3** and the trimethoxy compound **11**. Only complex mixtures of substitution products were obtained. Using the same acetylation and protonation scheme used for formation of trinitrotriol follow by bromination it was possible to synthesize tris(5-bromo-2-hydroxy-phenyl)amine



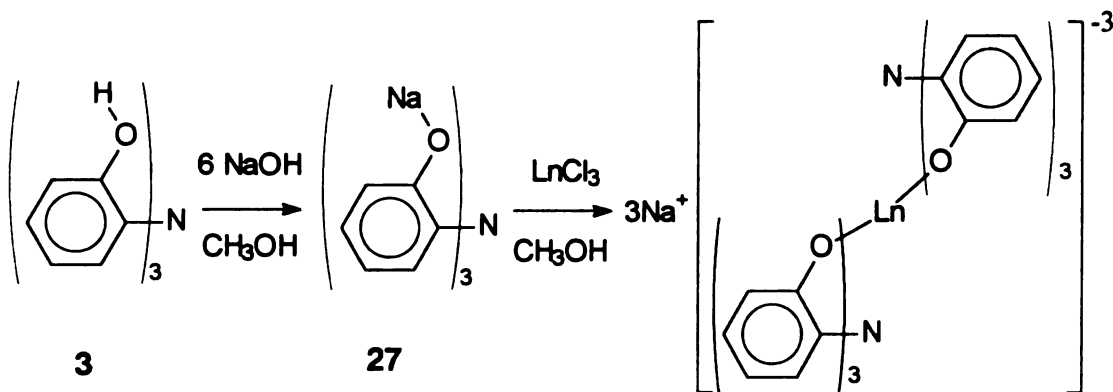
(bromotriol) **36**. The bromotriol was identified by NMR only and was never used for any complex formation. Exhaustive bromination yielded the symmetric product **25** (<25%), a hexabromo trimethoxy triphenyl amine. Unfortunately upon demethylation the resulting hexabromotriol **26** was only sparingly soluble in most

organic solvents. Due to the poor solubility and low yield of this reaction, this direction of study was not pursued further.

2.2. Synthesis of Complexes

Lanthanides in the presence of hydroxides usually make an insoluble polymeric material. Therefore, we first attempted to synthesize the 1:1 lanthanide triolate complexes in anhydrous acetonitrile using sodium hydride as a base. This procedure resulted in insoluble solids (later identified as the 1:1 complexes) and dark blue solutions. The blue color might indicate anionic or polyanionic radical species, but attempts to isolate and purify the blue compounds were unsuccessful.

Scheme 2.4

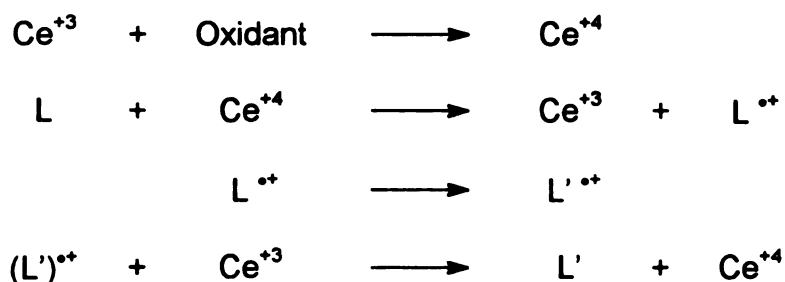


Difficulties in the synthesis of neutral 1:1 complexes led us to explore the charged 2:1 complexes with the general formula $\text{Na}_3\text{Ln}(\text{triolate})_3 \cdot n\text{H}_2\text{O} \cdot m\text{CH}_3\text{OH}$. Addition of a methanolic solution of lanthanide(III) chloride to a clear colorless solution of sodium triolate **27** resulted in a clear solution. But with ratios of triolate to lanthanide less than 2:1, white precipitates formed corresponding to the 1:1 complexes. Concentration of the remaining solution led to crystallization

of the 2:1 complexes. Using similar procedures, we isolated the lanthanum, gadolinium, and ytterbium 1:1 (**28**, **29**, **30**) and 2:1 (**31**, **32**, **33**) complexes.

Attempts to isolate a cerium complex failed. The reaction mixture would turn dark brown to black followed by the precipitation of unidentified tar. This result may be due to the ease of oxidation of Ce^{+3} in the presence of oxy-bases.⁴ The smallest trace of oxidant may start a cycle of auto-oxidation where the Ce^{+4} oxidizes the ligand, which after undergoing further changes could oxidize a Ce^{+3} ion (Scheme 2.5). The radical cation of the ligand is not stable, and its formation would lead to destruction of the ligand and the formation of tar. No attempt was made to identify the oxidation products from this reaction.

Scheme 2.5:



2.3. NMR Analysis

The presence of a strong paramagnetic center hinders NMR analysis of lanthanide complexes by causing broadening and shifting of the proton signals. However, lanthanum itself is diamagnetic and does not present this difficulty. In addition, although ytterbium ($s = \frac{1}{2}$) is paramagnetic and causes large proton chemical shifts, it does not broaden and shift signals as much as gadolinium

($s=7/2$). Therefore NMR can help in the characterization of both lanthanum and ytterbium complexes.

The NMR spectra seen in Figure 2.1 show the proton signals in the triolate **27** shifted upfield from the free triol **3** (not shown) at 7.0–6.86 ppm, as expected. When the triolate forms a complex with lanthanum **31**, the proton signals shift back downfield, consistent with the expected electron density depletion from the ring. The titration of sodium triolate **27** with lanthanum chloride in D₂O, Figure 2.2, shows clearly that there is a 2:1 complex. At ratios of less than 2:1, NMR becomes close to impossible because precipitate formation interfered with the lock signal. The presence of two distinct sets of signals, for the triolate and the complex, and the fact that lowering the temperature to 5°C from 25°C showed no significant line width or chemical shift variation of any of the signals, together indicate that this complex does not undergo ligand exchange on the NMR timescale.

Titration of the trinitro triolate **37**, (triple deprotonated **18**) with LaCl₃ in D₂O also provided evidence for 2:1 complexation through broadening and shifting of signals, but there were no distinct free and complexed trinitrotriolate signals. Attempts to resolve the proton signals by variable temperature NMR to get complexation rates proved unsuccessful within the accessible temperature range, but the complexation rate appears to be fast on the NMR timescale. On the other hand in methanol solution, two distinct sets of signals were observed which showed no significant line width or chemical shift variation of any of the signals even at -100°C.

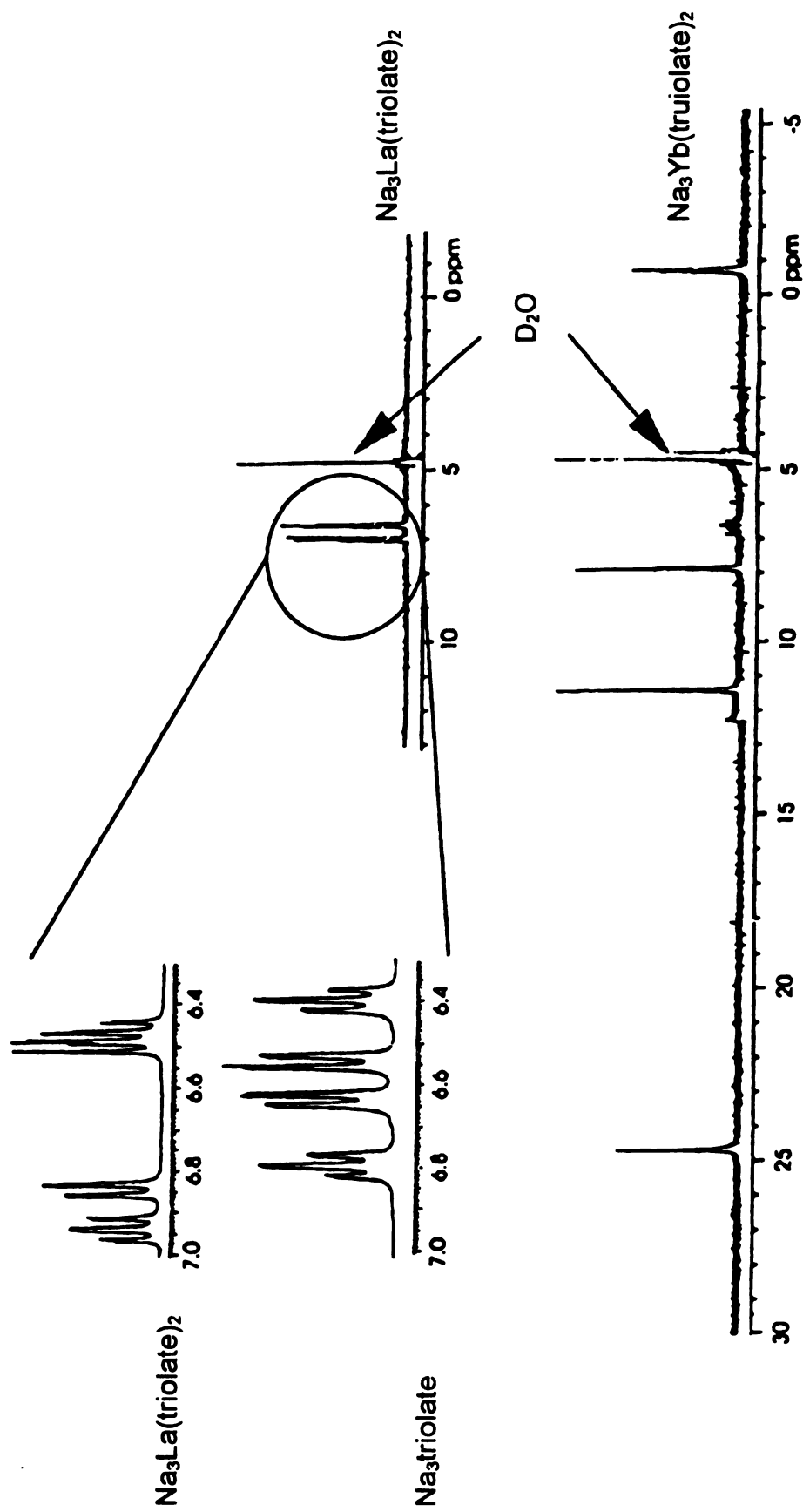


Figure 2.1: ^1H -NMR spectra of $\text{Na}_3\text{triolate}$ **27**, $\text{Na}_3\text{La}(\text{triolate})_2$ **31**, and $\text{Na}_3\text{Yb}(\text{triolate})_2$ **33** in D_2O

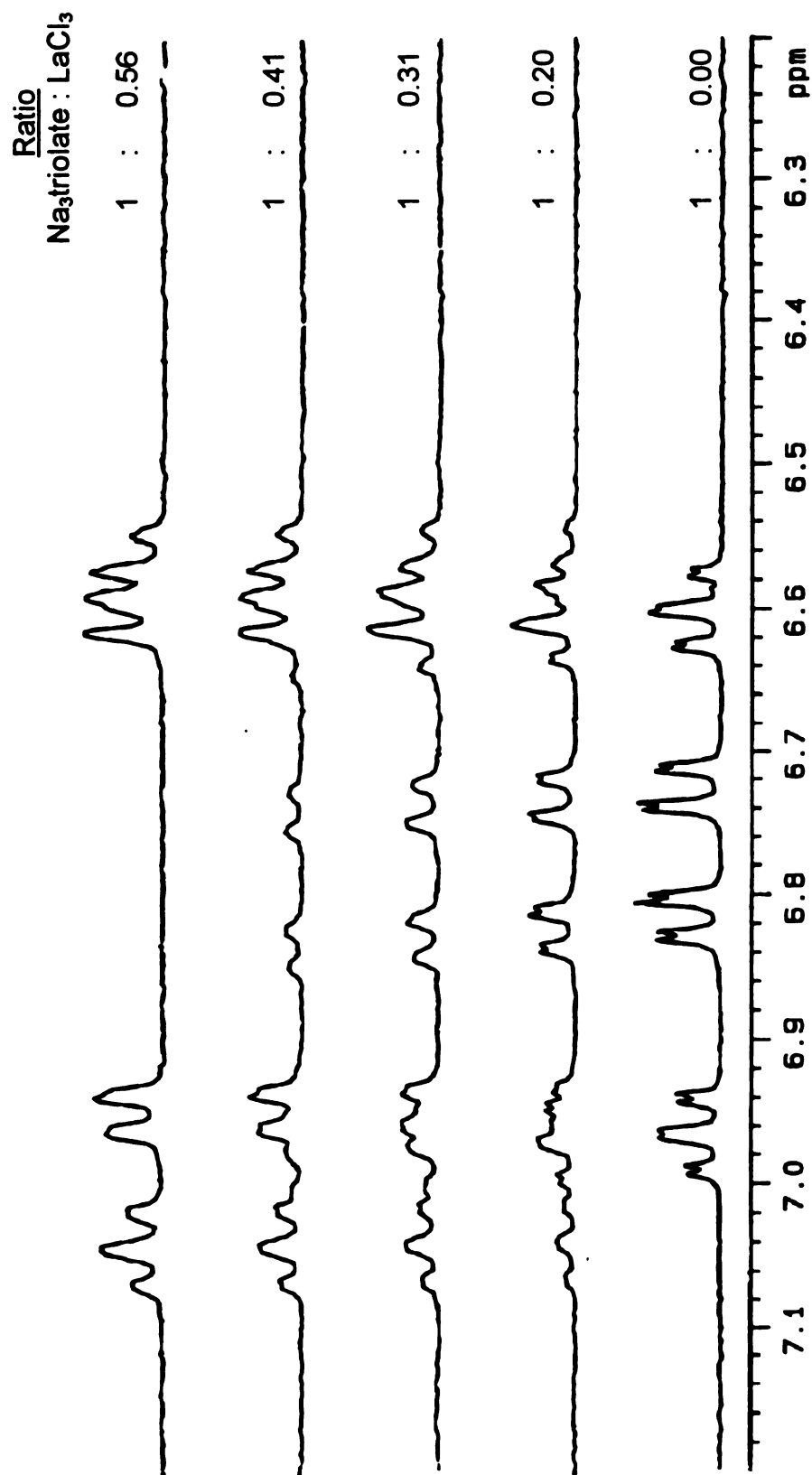


Figure2.2: ¹H-NMR spectra of Na₃triolate **27** titrated with La Cl₃ in D₂O

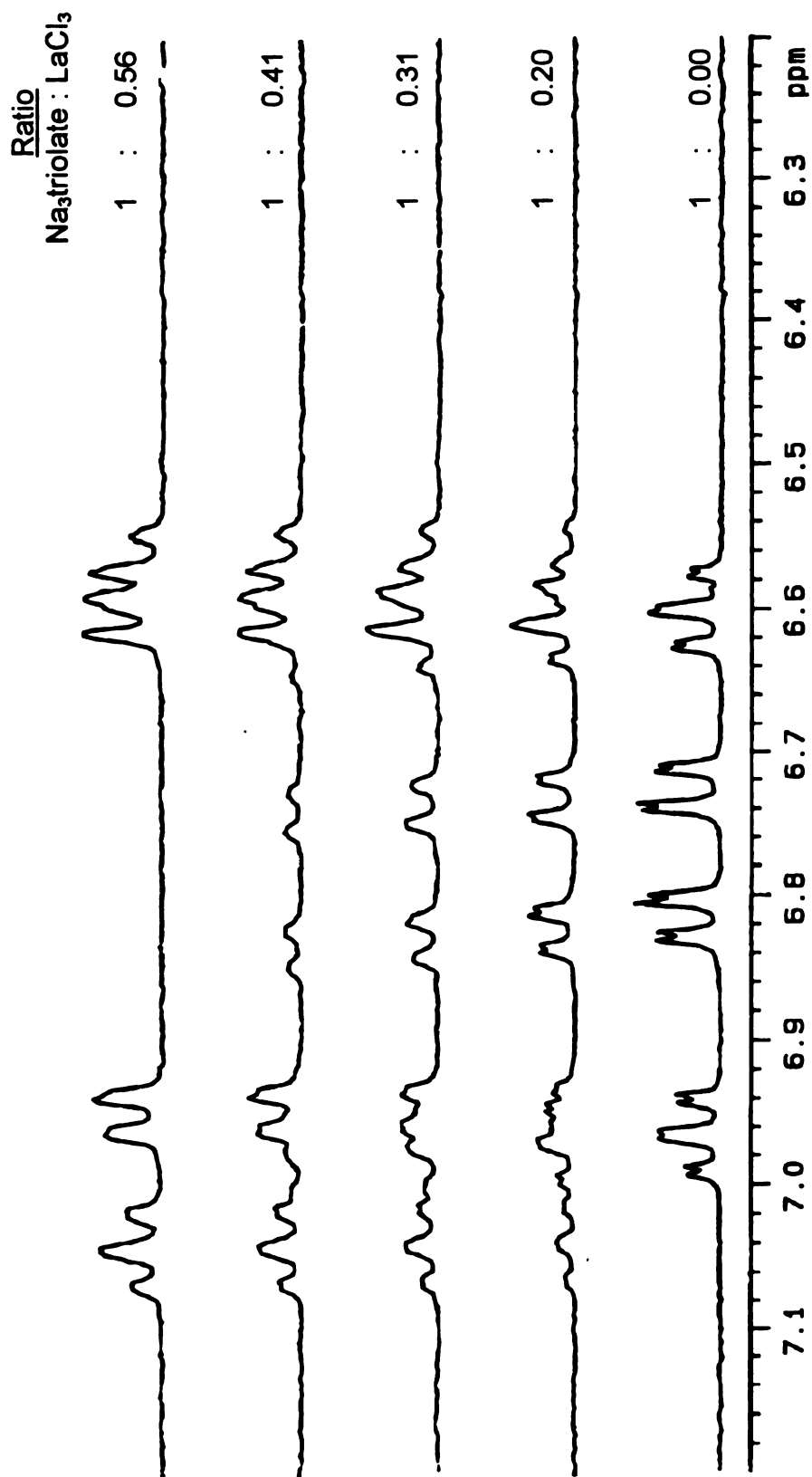


Figure2.2: ¹H-NMR spectra of Na₃triolate **27** titrated with La Cl₃ in D₂O

This behavior led us to conclude that in methanol the exchange happens much slower than the NMR timescale.

A first look at the NMR spectrum of the ytterbium triolate complex **33** in D₂O showed only two signals at 7.90 and 11.4 ppm, but expansion of the scale uncovered the other two signals at 24.5 ppm and at -0.5 ppm. Titration analysis showed that the Yb complex **33**, like the La complex **31**, had a 2:1 stoichiometry and had no appreciable exchange at the NMR timescale.

2.4. Mass Spectrometric Analysis

The stability of lanthanide triolates shown in the NMR studies led us to examine them by mass spectral analysis. Using negative ion fast-atom-bombardment mass spectrometry (FABMS), on a recrystallized sample of complex **31**, it was possible to observe the molecular ion of the La(triolate)₂ nucleus at m/z 721. This included 2 protons, and had a charge of -1. Such protonation is not unexpected, given the hydrogen-rich glycerol matrix used to volatilize the sample. The peak at m/z 520.2 is due to the 1:1 complex with one monodeprotonated glycerol attached, while the peak at m/z 446.1 corresponds to the 1:1 complex with a hydroxide attached. From these data, it is not clear if there is a mixture of 1:1 and 2:1 complexes in the matrix, or if these two peaks are fragmentation products of the 2:1 complex. It might be possible to test the latter case using tandem mass spectrometry to isolate the molecular ion peak, but we did not have the opportunity to conduct such an experiment.

2.5. X-ray Structures

Crystals of the 1:1 complexes of lanthanum **28** and gadolinium **29**, and 2:1 complexes of gadolinium **32** and ytterbium **33** have been analyzed by X-ray diffraction. Selected geometrical data are compared in Table 2.1

Table 2.1: Bonds and Angles of Lanthanide Triolate Complexes

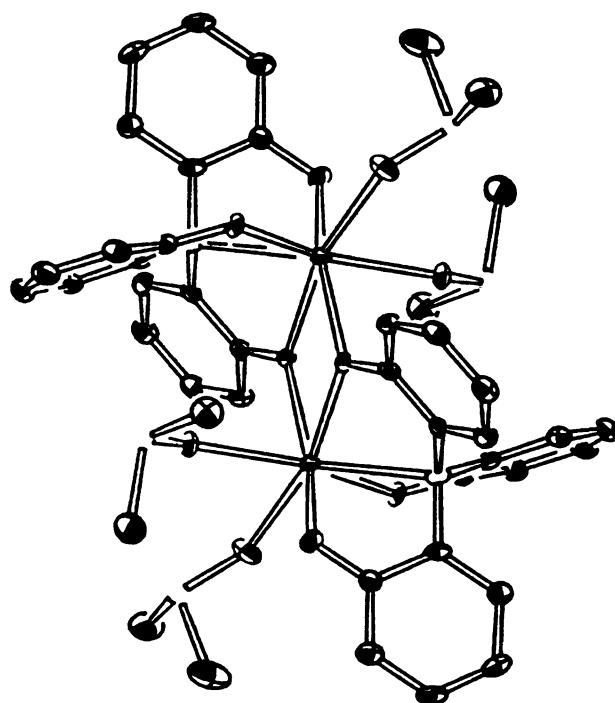
	La 1:1 28 ^a		Gd 1:1 29	Gd 2:1 32	Yb 2:1 33 ^b	
Ln-Ln	3.974(3)		3.8719(8)	7.802(5)	7.744(1)	7.842(1)
Ln-OPh^c	2.34(2)	2.40(2)	2.239(3)	2.353(7)	2.322(8)	2.296(8)
	2.37(2)	2.47(2)*	2.311(3)	2.364(8)	2.283(7)	2.33(1)
	2.57(2)*	2.44(2)	2.336(3)*	2.401(8)	2.289(9)	2.293(8)
bridging OPh	2.44(2)	2.66(2)	2.361(3)			
average Ln-OPh	2.44	2.49	2.312	2.37	2.30	
Ln-DMSO	2.64(2)	2.56(1)	2.365(3)			
	2.56(2)	2.65(1)	2.372(3)			
		2.57(1)				
bridging Ln-DMSO	2.66(1)	2.72(1)				
average Ln-DMSO	2.618	2.623	2.369			
Ln-N	2.80(2)	2.92(2)	2.630(4)	2.667(9)	2.66(1)	2.66(1)
pyramidalization angle^d	104.2	105.7	104.2	105.4	104.9	104.9
N-Ln-N angle				160.8(4)	158.9(2)	
ring twist ring 1	57.6(9)	74.4(7)	63.6(2)	52.9(5)	60.8(5)	74.0(4)
	61.7(6)	66.4(7)	58.5(2)	71.4(5)	75.8(4)	59.5(5)
	70.9(8)	57.3(9)	70.6(2)	59.5(4)	53.4(5)	52.8(4)

^aFirst column refers to La(triol) with Coordination Number (CN)=8 second column La(triol) CN=9; ^b columns represent different triolate caps; ^cListed in order of increasing label number; * indicates bridging OPh; ^d Pyramidalization angle is defined as $90 + \sin^{-1}(\text{average CN distance} / \text{Displacement of N from CCC plane})$

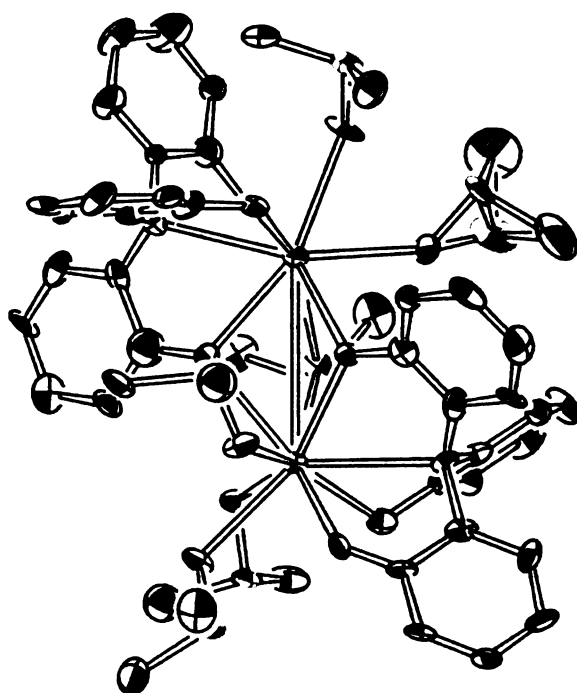
Crystallographic data for these compounds can be found in Tables A1-4, while their fractional coordinates and anisotropic displacement parameters are given in Tables A5-12 in the Appendix. Drawings with atom-labeling schemes are given in Figures A5-A8. Examination of the 2:1 complexes of gadolinium **32** and ytterbium **33** crystals was incomplete, because, in each case the crystal fell off the sample mount 2/3 of the way through the data collection (Extreme building vibrations caused by construction occurred over the 2-3 weeks of data collection.) Fortunately, the remaining data sets were of sufficient quality to yield reasonable structures, but refinement of the thermal parameters using full-matrix least-squares on either F or F^2 resulted in some non-positive-definite atoms.

As expected, the X-ray data pointed to two unique structural motifs, corresponding to the 1:1 and 2:1 complexes. The 1:1 complexes exist as dimers with the triolates bridging two lanthanides in the crystal. These are isolated dimers with no close intermolecular contacts or any uncoordinated solvent molecules in the structure. The 2:1 structures consist of a core lanthanide triolate "sandwich", one lanthanide capped with two triolates. The sodium counterions connect these trinegative ions into parallel chains, with all the metals in the same plane.

The 1:1 lanthanum and gadolinium complexes (Figure 2.3) showed a dimer structure similar to the aluminum complex **6a**. The lanthanum complex is asymmetric with coordination numbers (CN) 8 and 9 at the two distinct lanthanum centers.



29



28

Figure 2.3: ORTEP drawings of (LaTriolate)₂•6DMSO **28** and (GdTriolate)₂•4DMSO **29**

The two lanthanum ions are 3.974(3) Å apart; each is capped by a triolate ligand. One phenoxide oxygen atom from each ligand and one oxygen atom from a DMSO molecule form a threefold bridge between the two metal centers. The remaining sites on the La centers are filled with three DMSO molecules on one La and two on the other. The average La -OPh distances are 2.44 and 2.49 Å respectively, with the longer distance found on the 9-coordinate La center. This is comparable to the La-OPh distances reported by Freeman et al.¹⁹ in their gadolinium catecholate dimers **13**. The central nitrogens are pyramidalized inward with pyramidalization angles ($90 + \sin^{-1}$ (average CN distance / displacement of N from the CCC plane, planar = 90°) of 104.2 and 105.7 respectively, with the larger angle found on the 9-coordinate La center. Stoudt et al.²⁶ reported similar pyramidalization in tris(2-alkoxyphenyl) amine complexes with sodium and potassium. Each ligand cap has a pseudo-C3 symmetry with a ring twist angle (the mean angle of aryl ring planes out of the central nitrogen's three-carbon plane; coplanar = 0.0 °) of 57.6(9), 61.7(6), 70.9(8) and 74.4(7), 66.4(7), 57.3(9). The La-N distances are 2.80(2) and 2.92(7) Å, significantly longer than other amine-La complexes in the literature. This long La-N distance may result from the larger lanthanum ion not fitting in the pocket or the fact that oxygen ligands have met the coordination requirements of the lanthanum ion and the non-basic nitrogen does not have much to offer in addition.

The Gadolinium 1:1 complex **29** has a similar structure to the lanthanum 1:1 complex **28**, except that it is symmetric, with a point of inversion between the two metal centers. Each Gd has a CN of 7. There are two triolate ligands, each

capping a gadolinium, with one of the phenoxides of each ligand bridging the two metal centers. The remaining sites on the gadolinium centers are filled with two DMSO molecules. The average for all Gd-OPh distances is 2.31 Å. This distance is shorter than in the lanthanum complex as expected, considering the smaller size of the gadolinium ion. The Gd-Gd distance is 3.8719(8) Å, shorter than 3.98 Å found by Liu et al. in their phenoxylate bridged dimer **14**.²⁷

The Gd 2:1 and Yb 2:1 complexes **32** and **33** have a core where the lanthanide is encapsulated between two triolates with no solvent oxygens coming close to the central metal. In these complexes the triolate acts as a tetradentate ligand with the central nitrogen also complexing the metal. These trianionic lanthanide sandwiches are connected in chains through the charge balancing sodium ions and solvents of crystallization.

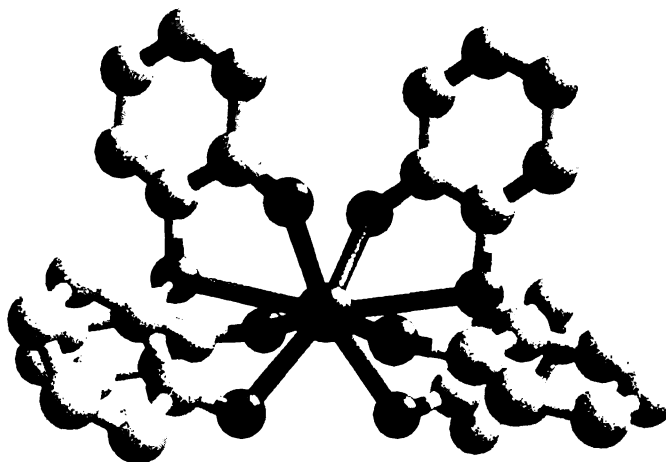


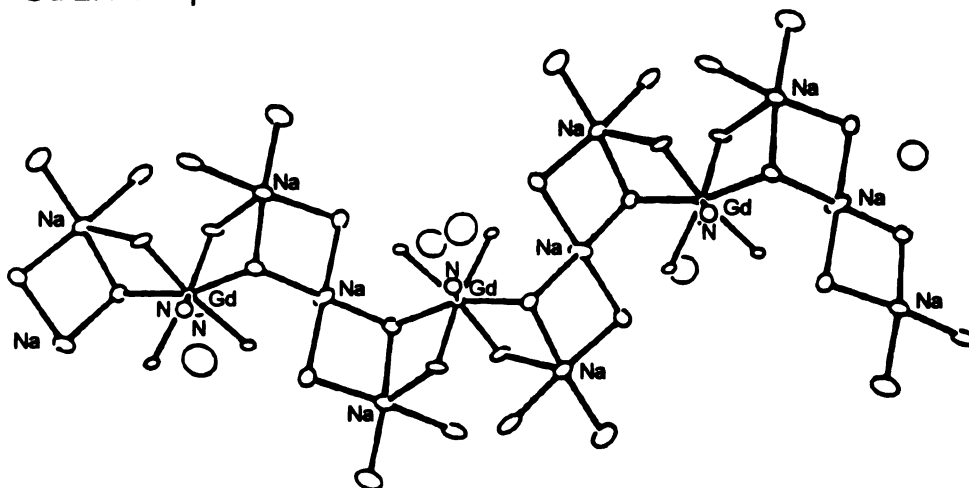
Figure 2.4: Core structure of $\text{Na}_3\text{Gd}(\text{triolate})_2 \cdot 2\text{H}_2\text{O} \cdot 6\text{CH}_3\text{OH}$ **32** clearly showing the diaratrane cage.

The sandwich complex shown in Figure 2.4 has the triolate caps off-center resulting in a N-Gd-N angle of 160.8(4)°; the Yb complex **33** has a similar

structure, with a N-Yb-N angle of $158.9(2)^{\circ}$. A similar offset of 154.5° has been reported by Stoudt et al. in their sodium tetraphenylborate salt complex with trimethoxytriphenyl amine **11**.²³ For gadolinium and ytterbium complexes **32** and **33** respectively, (see Table 2.1), the average Ln-OPh distances are 2.37 Å and 2.30 Å; For Gd and Yb complexes **32** and **33** respectively, the average Ln-OPh distances are 2.37 and 2.30 Å; the Gd complex **32** has a C₂ axis through the Gd center; the triolate-Ln cages have pseudo-C₃ symmetry with ring twists angles of $52.9(5)^{\circ}$, $71.4(5)^{\circ}$, $59.5(4)^{\circ}$ for Gd complex **32** and $60.8(5)^{\circ}$, $75.8(4)^{\circ}$, $53.4(5)^{\circ}$, $74.0(4)^{\circ}$, $59.5(5)^{\circ}$, $52.8(4)^{\circ}$ for Yb complex **33**; and the central nitrogens are pyramidalized inward with pyramidalization angles of 105.4° in the Gd complex, and 104.9° and 104.9° in the Yb complex (see Table 2.1).

As shown in Figure 2.5 the extended structures consist of chains of lanthanide triol sandwiches connected through sodium ions. The sandwiches alternate opening slightly to the outside of the chain, left and right. There are three sodium ions in a line between each sandwich. The central sodium ion is connected to one phenoxide of each sandwich. All the metal ions (Na⁺ and lanthanide) in a single chain lie in the same plane. In the end-on view (Figure 2.6) one can see that the Yb 2:1 complex **33** has a slight twist to the chains.

Gd 2:1 complex **32**



Yb 2:1 complex **33**

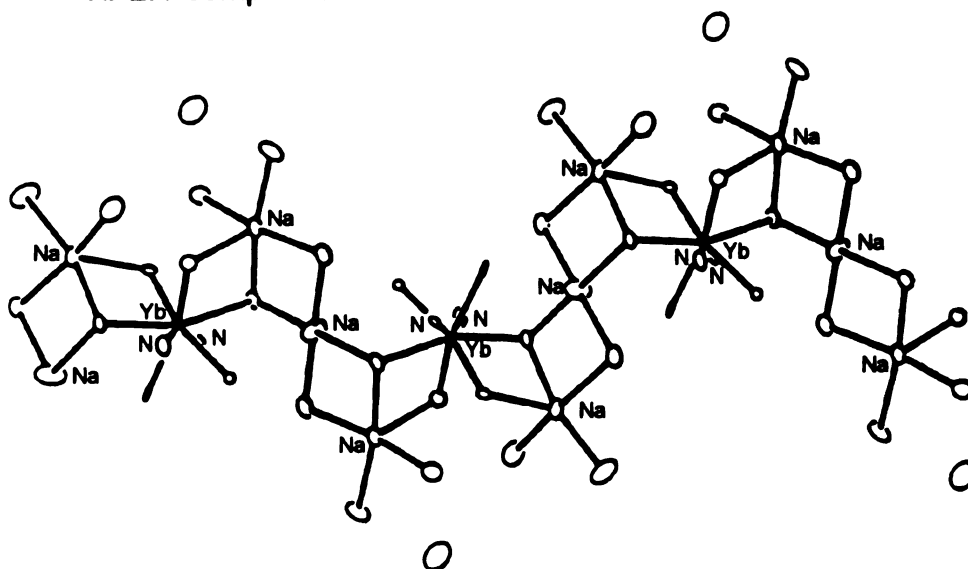
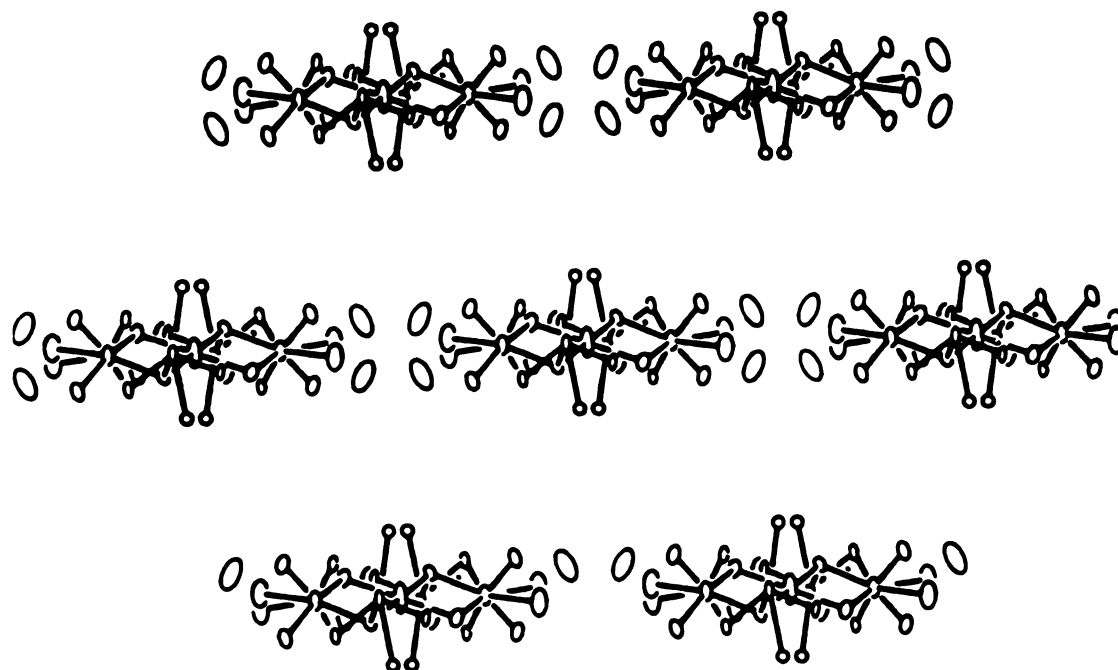


Figure 2.5: Views perpendicular to the metal-containing plane of $\text{Na}_3\text{Gd}(\text{triolate})_2 \cdot 2\text{H}_2\text{O} \cdot 6\text{CH}_3\text{OH}$ **32** and $\text{Na}_3\text{Yb}(\text{triolate})_2 \cdot 2\text{H}_2\text{O} \cdot 5\text{CH}_3\text{OH}$ **33** (carbon and hydrogen atoms are omitted for clarity).

Gd 2:1 complex **32**



Yb 2:1 complex **33**

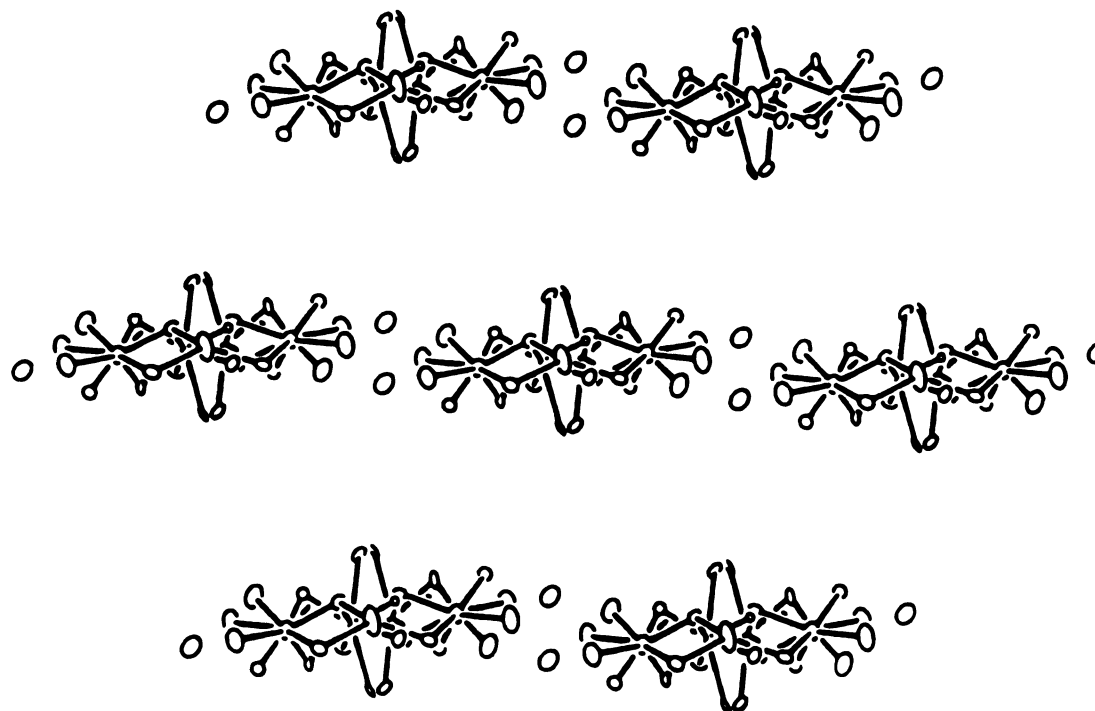


Figure 2.6: End on views of $\text{Na}_3\text{Gd}(\text{triolate})_2 \cdot 2\text{H}_2\text{O} \cdot 6\text{CH}_3\text{OH}$ **32** and $\text{Na}_3\text{Yb}(\text{triolate})_2 \cdot 2\text{H}_2\text{O} \cdot 5\text{CH}_3\text{OH}$ **33** (carbon and hydrogen atoms are omitted for clarity).

2.6. Magnetic Studies

Magnetic susceptibility measurements in the temperature range from 1.8 K to 300 K and -200 G to 50 kG were performed on a MPMS Quantum Design SQUID magnetometer., Figure 2.7 shows the temperature dependence of the magnetic susceptibility's, displayed as the product (χT), for the 2:1 and 1:1 complexes of Gd and Yb. The Gd 2:1 complex **32** has a steady χT of $7.5 \text{ cm}^3 \text{ K mol}^{-1}$ between 300 K and 70 K. Below 70 K, χT increases slightly to a value of $7.85 \text{ cm}^3 \text{ K mol}^{-1}$ at 10 K and then more rapidly to a maximum of $8.12 \text{ cm}^3 \text{ K mol}^{-1}$ at 5 K. Below 5 K χT decreases to $7.5 \text{ cm}^3 \text{ K mol}^{-1}$ at 1.8 K. This low temperature rise could result from ferromagnetic coupling in the chains. If this is true however, the coupling would be extremely small. More data are needed to verify that this is a real magnetic phenomenon. The decrease below 5 K could be a result of antiferromagnetic coupling between the gadolinium ions.

The Yb 2:1 complex **33** shows a steady decrease in χT from $1.36 \text{ cm}^3 \text{ K mol}^{-1}$ at 300 K to $1.27 \text{ cm}^3 \text{ K mol}^{-1}$ at 10 K. Below 10 K, χT increases to $1.43 \text{ cm}^3 \text{ K mol}^{-1}$ at 1.8 K. This behavior may result from ferromagnetic coupling in the chains, but the complexity of the magnetic behavior of Yb limits realistic speculation as to the nature or mathematical fitting of the interactions. Similar to the Yb 2:1 complex **33**, the Yb 1:1 complex **30** shows a steady decrease in χT from $3.17 \text{ cm}^3 \text{ K mol}^{-1}$ at 300 K to $2.3 \text{ cm}^3 \text{ K mol}^{-1}$ at 6 K. Below 6 K, χT decreases sharply to $1.8 \text{ cm}^3 \text{ K mol}^{-1}$ at 1.8 K. This decrease suggests modest antiferromagnetic coupling, as might be expected when two paramagnets are placed in close proximity. A final note on the Yb complexes is that the room

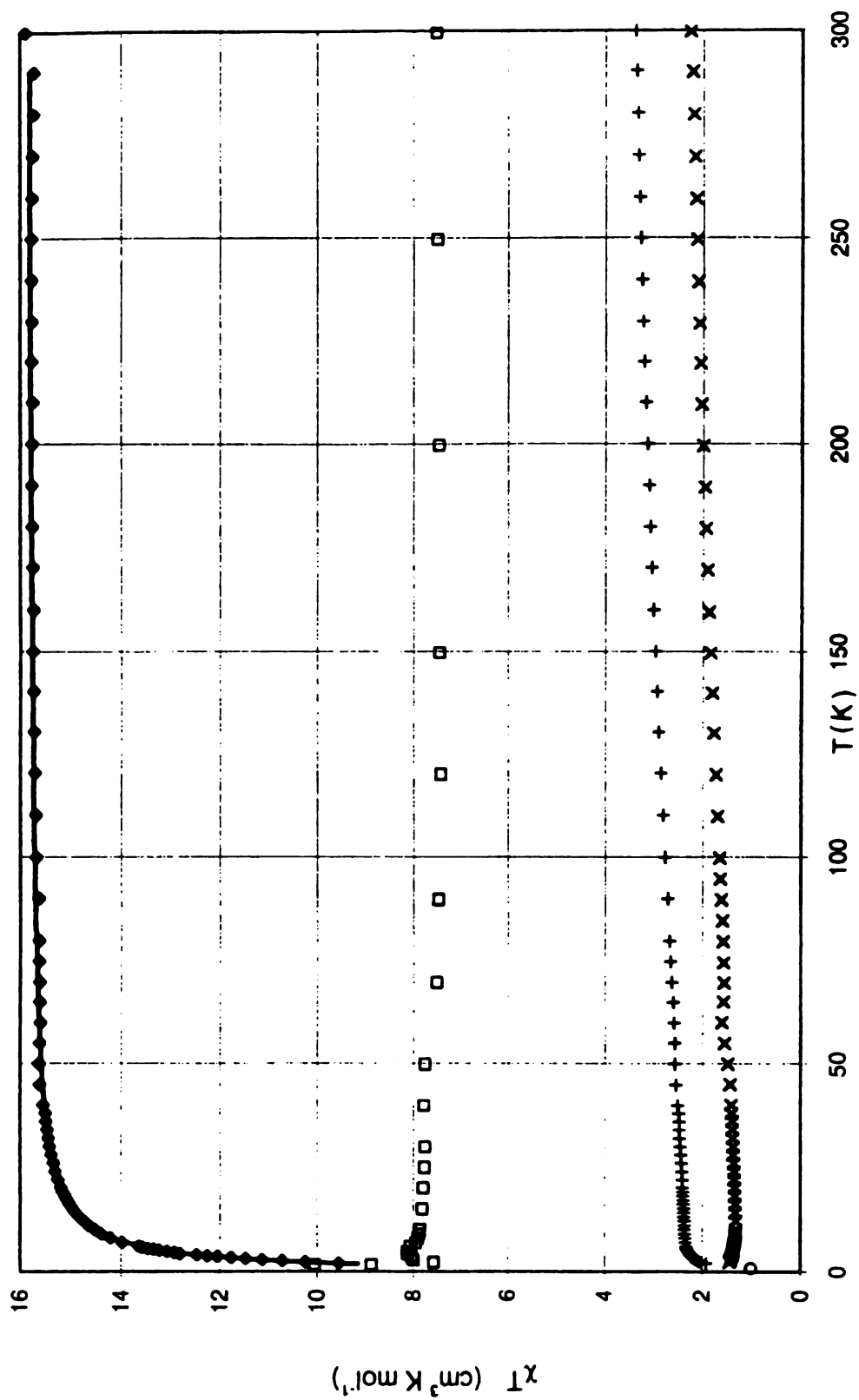


Figure 2.7: χT vs T curves for (●) $\text{Gd}_2(\text{triolate})_2 \cdot 4\text{DMSO}$ **29**; (□) $\text{Na}_3\text{Gd}(\text{triolate})_2 \cdot 2\text{H}_2\text{O} \cdot 6\text{CH}_3\text{OH}$ **32**; (+) $\text{Yb}_2(\text{triolate})_2 \cdot 4\text{DMSO}$ **30**; (x) $\text{Na}_3\text{Yb}(\text{triolate})_2 \cdot 2\text{H}_2\text{O} \cdot 5\text{CH}_3\text{OH}$ **33** (---) calculated fit for Gd 1:1 **29**.

temperature χT values are approximately one-half of the theoretically predicted values using the free-ion approximation 2.57 and 5.14 cm³ K mol⁻¹ for the 2:1 and 1:1 complexes, respectively. These numbers however, are based on an assumed formula Na₃Yb(triolate)₂•2H₂O•5CH₃OH and (Yb-Triolate)₂•4DMSO. These formulas are obtained from the X-ray structures; no elemental analyses were done.

The Gd 1:1 complex **29** shows a χT of 15.8 cm³ K mol⁻¹ at 300 K which is quite close to the free-ion predicted value of 15.76 cm³ K mol⁻¹. The value of χT decreases slowly to 15.6 cm³ K mol⁻¹ at 50 K. Below 50 K there is a progressive decrease to 9.15 cm³ K mol⁻¹ at 1.8 K. Gadolinium has a ⁸S ground state which allows an expression to be derived for the magnetic susceptibility using the Hamiltonian $H=J S_1 S_2$.

$$\chi_{t,j} = \frac{\left[\sum_s S(S+1)(2S+1)\Omega_s e^{\left(\frac{-W_{S,j}}{kT_t}\right)} \right]}{T_t \left[\sum_s (2S+1)\Omega_s e^{\left(\frac{-W_{S,j}}{kT_t}\right)} \right]} 0.125048612 g^2$$

$$g = 2$$

$$s = 7/2$$

$$S = 2s, 2s-1, \dots, 0$$

$$W_{S,j} = J_s (S(S+1) - 2S(S+1))$$

$$\omega_s = 2s+1-S$$

$$\Omega_s = \omega_s - \omega_{(s+1)}$$

Equation 2.1: Equation for the magnetic susceptibility of two coupled S=7/2 ions.

This model has two 7/2 spins coupled antiferromagnetically where J is the coupling constant. A least squares fit of the experimental data using Equation 2.1²⁸ yields an antiferromagnetic coupling constant $J = -0.058 \text{ cm}^{-1}$ and $g = 2.0$. Table 2.2 lists coupling constants for gadolinium dimeric systems. From the literature data it can be seen that our $J = -0.058 \text{ cm}^{-1}$ is in the lower range. This is comparable to $J = -0.053 \text{ cm}^{-1}$ determined by Panagiotopoulos et al.¹⁹ in their acetate-bridged Gd complex, but is higher than the $J = -0.045 \text{ cm}^{-1}$ reported by Liu et al.¹⁸ One thing to note is that Liu's phenoxide-bridged complex has a longer Gd-Gd distance (3.98 Å) than the 3.87 in our Gd 1:1 complex **29**. It would be expected that the shorter Gd-Gd distance would result in stronger magnetic coupling.

Table 2.2 Magnetic coupling constants for gadolinium dimer complexes.

Bridging atom type	Gd-Gd (Å)	$J \text{ (cm}^{-1}) / g$	Ref.
Carboxylate (system has Zn^{+2} ions in the structure)	4.2515(2)	-0.042 / 2.0	29
Phenoxy	3.98	-0.045 / n/a	20
Acetate	<4.0	-0.053 / n/a	21
Phenoxy (Gd 1:1 29)	3.8719(8)	-0.058 / 2.0	
Alkoxy (three Gd ions in equilateral triangle)	3.730(2)	-0.092 / 1.98	24
Phenoxide (schiff base)	n/a	-0.104 / 1.999	23
Phenoxide (schiff base)	n/a	-0.140 - -0.082 / n/a	30
isophthalate	n/a	-0.18 / n/a	31
isophthalate	n/a	-0.19 / n/a	32
Alkoxy	3.7643(7)	-0.198 / 1.975	33
isophthalate	n/a	-0.21 / n/a	34
Phenoxy (schiff base)	3.6353(2)	-0.22 / 1.93	35
Phenoxy (schiff base)	n/a	-0.240 / n/a	22
Benzoate	n/a	-0.471 / 1.975	36

In summary, triol **3** and trinitrotriol **16** react with LnCl_3 in the presence of sodium hydroxide to form 1:1 and 2:1 complexes as shown by the crystal structures of complexes **28**, **29**, **30**, and **31** and NMR analysis of complexes **31** and **33**. Magnetic studies of the Gd 1:1 complex **29** have shown antiferromagnetic coupling between the gadolinium ions with $J = -0.058 \text{ cm}^{-1}$. This weak coupling is typical of dimeric lanthanide complexes, due to the small radial extent of the magnetically active f orbitals. It suggests that the coupling between more widely separated centers would quickly become negligible, in agreement with the magnetic data for the 2:1 complexes, which show at most hints of coupling. These findings cast doubt on the potential of lanthanide triolate complexes as building blocks to make extended magnetic structures. On the other hand, the presence of the triply sodium-bridged chains in the 2:1 complex suggest that such complexes with other, more strongly interacting, paramagnetic metals might develop nontrivial intercluster coupling, as seen in the work of Misiolek, et al. from this research group.³⁷ Trinitrotriol **16** shows promise as a stable, oxidation-resistant ligand, and merits further investigation.

EXPERIMENTAL

Figures 2.3 and 2.4 are presented in color.

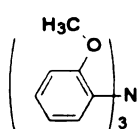
3.1. Equipment and Chemicals used

All manipulations were performed either in a glove bag continuously purged with N₂ or on a low vacuum Schlenk line that pumped to 1 torr and was directly attached to an argon tank with no scrubbing columns for deoxygenation. Solutions were purged with N₂ or argon for at least 10 min. Glassware was generally soaked in a base bath (NaOH isopropanol) for at least one day, then rinsed with deionized (DI) water, dipped in an acid bath (aqueous 5-10% HCl), rinsed with DI water and then acetone, and allowed to air dry. All chemicals were reagent grade and were purchased from Aldrich. Melting points were determined on a Thomas-Hoover apparatus and are uncorrected.

Routine ¹H and ¹³C NMR spectra were obtained at 300 and 75 MHz, respectively, on Varian GEMINI 300 or VXR-300 spectrometers; the latter instrument was used for all variable temperature (VT) analysis. ¹H NMR shifts reported herein are referenced to residual ¹H resonances in deuterated solvents: acetone-d₆ (δ 2.04 ppm); CDCl₃ (δ 7.24 ppm); D₂O (δ 4.66 ppm); and methanol-d₄ (δ 3.30 ppm for the CD₃ group). The ¹³C shifts are referenced to those of the deuterated solvent CDCl₃ (δ 77 ppm) and methanol-d₄ (δ 49 ppm). Peak multiplicities are abbreviated: s, singlet; d, doublet; t, triplet; dd, doublet of doublets; m, multiplet.

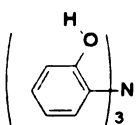
3.2. Synthesis:

3.2.1. Ligands



Tris(2-methoxyphenyl)amine 11 was prepared using Frye's procedure⁶ except that 18-crown-6 was used as described below. A

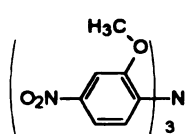
500 ml three-neck round-bottom flask fitted with a mechanical stirrer was charged with 12.3 g (0.1 mol) of anisidine, 51 g (0.22 mol) of 2-iodoanisole, (100 g, 0.72 mol) of K₂CO₃, 28 g (0.44 mol) of electrolytic copper and 5 g (0.019 mol) of 18-crown-6. After the addition of 200 ml 1,2-dichlorobenzene the flask was fitted with a condenser. The reaction was allowed to reflux for 48 hours, after which TLC showed complete conversion to the triarylamine **11**. The reaction was allowed to cool to room temperature and was taken up in chloroform. The solid was filtered off, and the chloroform and 1,2-dichlorobenzene removed by rotary evaporation, resulting in a brown-black tar. Addition of 100 ml acetone, followed by cooling overnight, led to precipitation of a white solid, which was filtered off and recrystallized from ethyl acetate. Several crops yielded 24.3g (73%) of product with mp 142-143.5 °C uncorrected (lit. 145-147 °C)⁶; H-NMR in CDCl₃; δ(ppm) 7.0 (m, 3H), 6.85-6.75 (m, 9H), 3.55 (s, 9H); ¹³C-NMR in CDCl₃ δ(ppm) 153.1, 137.7, 124.5, 123.7, 120.6, 112.6, 55.7. EIMS m/z 335(M⁺).



Tris(2-hydroxyphenyl)amine (triol) 3 was prepared by dissolving

18.4 g (55.2 mmol) of tris(2-methoxyphenyl)amine **11** in 100 ml toluene in a 500 ml round-bottom flask to which 25 g (188 mmol) of AlCl₃ was then added. The mixture was refluxed for 4 hours. The mixture was quenched with 150 ml of 10% aqueous HCl, resulting in the precipitation of a gray-white

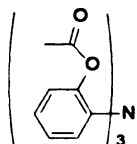
solid. This material was collected by filtration and recrystallized from methylene chloride to give 6.7 g of triol **3**. Additional product was recovered from the toluene layer by removal of the solvent under vacuum. The resulting brown solid was recrystallized from toluene. The two batches were combined after checking purity by NMR and recrystallized from toluene for a final yield of 11.2 g (76%) of triol. mp. 167.5-168.5°C (lit. 171-174°C⁶): ¹H-NMR in CDCl₃ δ(ppm) 7.09 (td, 3H), 6.86 (td, 3H) 6.94 (dd, 6H) ¹³C-NMR in CD₃OD δ(ppm) 152.48, 136.98, 126.70, 126.17, 120.94, 117.41 EIMS m/z 293 (M⁺).



Tris(2-methoxy-4-nitrophenyl)amine 21. 2-Methoxy-4-nitro-

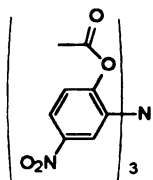
aniline **17** 50 g (0.3 mol) was converted to 2-iodo-5-nitro-anisole **18** using a standard literature procedure.³⁸ A 250 ml three-neck round-bottom flask fitted with a mechanical stirrer was charged with 1.68 g (10 mmol) 2-methoxy-4-nitroaniline **19**, 16.8 g (60 mmol) 2-iodo-5-nitro-anisole **20**, 10 g (72 mmol) K₂CO₃, 2.8 g (44 mmol) electrolytic copper and 0.5 g (1.9 mmol) 18-crown-6. After addition of 50 ml 1,2-Dichlorobenzene the flask was fitted with a condenser. The reaction was allowed to reflux for 3 days, after which TLC showed no more starting compounds. The reaction was allowed to cool to room temperature and was extracted with chloroform. The solid was filtered off, and the chloroform and 1,2-dichlorobenzene removed by rotary evaporation, resulting in a yellow-brown-black tar. The product were purified on a silica gel column using ethyl acetate/hexane (1:1) as solvent. The first compound to come off was 3-nitroanisole. The first yellow product (~30%) was bis(2-methoxy-4-nitrophenyl) amine **20**. ¹H-NMR δ (ppm) 7.93 (dd, 1H), 7.79 (d, 1H), 7.48 (d, 1H),

The second yellow product (~30%) was tris(2-methoxy-4-nitrophenyl) amine **21**. mp 191-195 °C uncorrected. $^1\text{H-NMR}$ in CDCl_3 δ (ppm) 7.79 (dd, 3H), 7.78 (s, 3H), 6.90 (d, 3H), 3.65 (s, 3H). EIMS m/z 470 (M^+)



Tris(2-acetoxyphenyl)amine 23. Triol **3** 6.0 g (20.5 mmol) was dissolved in 10 ml pyridine and 20 ml acetic anhydride. This mixture was refluxed for 2 hours. Ether (40 ml) was added, and the solution

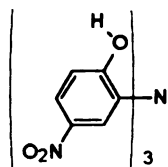
extracted with aqueous CuSO_4 until no more pyridine complex was visible as indicated by the lack of color change in the CuSO_4 layer. The ether was then removed under vacuum, resulting in 8.4 g (98% yield) tris(2-acetoxyphenyl) amine **21**, mp 130-132°C (lit.133-135)⁶. $^1\text{H-NMR}$ in CD_3OD δ (ppm) 7.05 (m, 12H), 1.67 (s, 9H). $^{13}\text{C-NMR}$ in CD_3OD δ (ppm) 168.7, 144.1, 138.7, 126.6, 126.4, 124.2, 123.8, 20.0



Tris(2-acetoxy-5-nitrophenyl)amine 22.

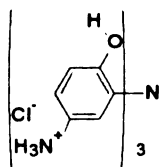
Tris(2-acetoxyphenyl)amine **21** (2.0 g 4.8 mmol) was dissolved in 20 ml acetic acid. Trifluoromethanesulfonic acid 1.5 ml (17 mmol) was added. In a separate flask, 5 ml concentrated nitric acid was dissolved in 10 ml acetic acid. Both solutions were cooled in an ice bath. The nitric acid solution was added dropwise to the triacetate solution over 20 min. A light yellow solid formed. The reaction was warmed up to room temperature and stirred for 1 hour, then 50 ml water was added and the yellow solid extracted with 3 times 50 ml portions of ether. After removal of the ether, the product was purified using a silica gel column. The third main yellow product from the column was identified as tris(2-acetoxy-5-nitrophenyl)amine **22**, 0.87 g (Yield 33%) mp

204-205 °C uncorrected. $^1\text{H-NMR}$ in CD_3OD δ (ppm) 8.18 (m, 6H), 7.36 (d, 3H), 1.82 (s, 9H). EIMS m/z 554 [M^+]. Note the other components were not positively identified but the complexity of their NMR spectra suggested an array of aryl ring substitution patterns.



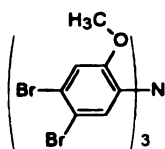
Tris(2-hydroxy-5-nitro-phenyl)amine 18. Tris(2-acetoxy-5-nitrophenyl)amine **24** (0.5 g 0.9mmol) was refluxed for one hour in 10 ml 0.45M NaOH in methanol. The reaction mixture was a deep

black-purple color. The reaction mixture was neutralized using 1M HCl, and an orange solid precipitated. This solid was collected and washed with water. No further purification was needed. Yield. 0.38g (98% yield) mp 256-258 °C $^1\text{H-NMR}$ in D_6 -acetone δ (ppm) 7.73 (m, 6H), 7.12 (d, 3H), 3.8 (s, 3H)



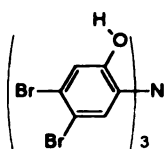
Tris(5-amino-2-hydroxyphenyl)amine-3HCl salt 34. Trinitro triol **18** (216 mg, 0.505 mmol) was dissolved in 8 ml of 2M NaOH under N_2 . 15 mg Pd/C 10%, 400 mg (10.5 mmol) NaBH_4 , and 10 ml H_2O

was added to a 40ml Schlink flask. The nitro triol solution was slowly added over a 10 min period. The reaction was stirred for another 30 min. The reaction mixture was then acidified, and the Pd/C filtered off. Adjusting the pH to ~7 resulted in the precipitation of a gray solid that was collected by filtration and was dried under vacuum. A small portion of this solid was dissolved in dilute HCl and allowed to dry, leaving the HCl salt **34**. (note: the NMR showed no other products) $^1\text{H-NMR}$ in D_2O δ (ppm) 6.85 (d, 3H), 6.78 (dd, 3H), 6.90 (d, 3H)



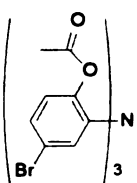
Tris(4,5-dibromo-2-methoxyphenyl)amine 25.

Tris(2-methoxyphenyl)amine **11** (200 mg, 0.60 mmol) was dissolved in 10 ml acetic acid. After the addition of 3 ml Br₂ the reaction was refluxed for 5 hours. A white solid formed and was filtered off, and identified as **25**. Yield not recorded. mp 278 (decomposes). ¹H-NMR in CDCl₃ δ (ppm) 7.35(s, 3H), 6.98 (s, 3H), 3.55 (s, 9H) (note: this spectrum show the presence of some other bromination products.) EIMS ^{m/z} 803, 805, 807, 809, 811, 813, 815 [M⁺].



Tris(4,5-dibromo-2-hydroxyphenyl)amine 26.

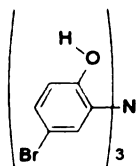
Tris(4,5-dibromo-2-methoxyphenyl)amine **25** (100 mg, 0.123 mmol) was dissolved in 10 ml toluene, and 0.2 g (15 mmol) AlCl₃ was added this mixture was refluxed for 3 h, then 10 ml 10% aqueous HCl was added. Filtration gave a white solid, which was almost insoluble in most organic solvents. Acetone did dissolve it enough to get a NMR spectrum. ¹H-NMR δ (ppm) 7.22 (s, 1H) 7.19 (s, 1H) OH 5.6 (~1H).



Tris(5-bromo-2-acetoxyphenyl)amine 35.

Tris(2-acetoxyphenyl)amine **23**, (200mg, 0.47 mmol), was dissolved in 8 ml acetic acid, and then 0.1ml (1.0 mmol) trifluoromethanesulfonic acid was added. A solution of Br₂ (0.2 ml) in 2 ml of acetic acid was added to the triacetate solution at 0°C. This mixture was allowed to warm up to room temperature and stirred for 1 hour. A white solid precipitated. The liquid was decanted, and the solid was washed with cold acetic acid and dried under

vacuum overnight. Yield was not determined. $^1\text{H-NMR}$ δ (ppm) 1.75 (s, 9H), 6.91 (dd, 3H), 7.25(m, 6H).



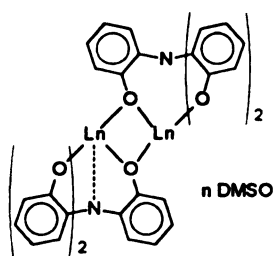
Tris(5-bromo-2-hydroxy-phenyl)amine 36 Tris(5-bromo-2-acetoxy-phenyl)amine **35**, (100 mg, 0.15 mmol) was placed in a Schlenk flask under an atmosphere of N_2 . To this was added 5 ml degassed 0.45M

NaOH in methanol. This mixture refluxed for 30 min. The reaction was acidified with 5 ml of degassed 10% HCl, resulting in the precipitation of a white solid.

The solid was extracted with ether. Yield was not determined. $^1\text{H-NMR}$ δ (ppm) 5.7 (br, 3H), 6.75 (d, 3H), 6.98 (dd, 4H), 7.06,(d, 3H).

3.2.2. Complexes

In the preparations of all complexes special efforts were made to exclude any air. Failure to do so resulted in the complex solutions turning black. All solutions were purged with dry N_2 for at least 10 minutes.

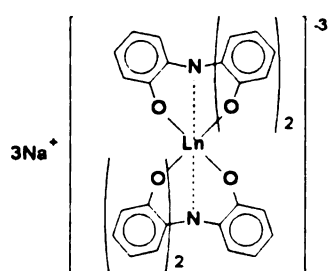


$\text{Ln}(\text{triolate}) \cdot n\text{DMSO}$ ($\text{Ln} = \text{La}$ **28**, Gd **29**, Yb **30**; $n=6,4,4$).

Triol **3**, 300 mg (1.02 mmol) was dissolved in 3.2 ml of 0.97M NaOH (3.1 mmol) in methanol. This solution was added to the appropriate $\text{LnCl}_3 \cdot x\text{H}_2\text{O}$ ($x=7,6,6$) lanthanide

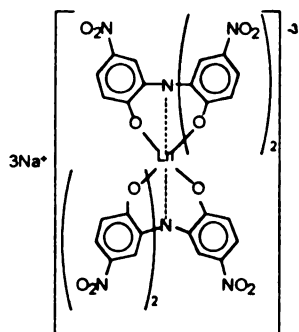
(1.0 mmol) salt in 18 ml of methanol. A precipitate formed immediately on adding the triolate **25** solution. The reaction was refluxed for 2 h, and then the solid was collected. The solid was dried under vacuum for at least 8 hours. Yields generally were approximately 80%. This 1:1 lanthanide-triolate complex was dissolved in 10 ml refluxing DMSO. On cooling, a white crystalline solid formed,

which was filtered and washed with cold DMSO and then dried under vacuum for 1 hour. Yield of the DMSO solvated complexes were generally greater than 80%. The Yb complex **28** was speculated to have 4 DMSO molecules based on thermo-gravimetric analysis kindly performed by the research group of Dr. Baker, which showed two losses corresponding to two DMSO molecules each.



Na₃(Ln)(triolate)₂•2H₂O•xCH₃OH (Ln = La **31**, Tb **37**, Gd **32**, Yb **33**; x=6,6,5,5) Triol **3**, (300 mg, 1.02 mmol), was dissolved in 10 ml methanol and 3.2 ml 0.97M NaOH (3.1 mmol) in methanol was added. To this

solution was added 0.5 mmol lanthanide salt in 5 ml of methanol. This reaction mixture was refluxed for 3 h. Note that complexes of the heavier lanthanide do not completely dissolve in this amount of methanol so 5 to 10 ml more methanol was added at reflux to form a clear solution. On cooling, needle-like crystals formed, in all cases except for lanthanum. The lanthanum complex formed only a microcrystalline solid. The solids were filtered and were **not** dried because they disintegrated when not in a saturated atmosphere of methanol. Yields generally were >90%, except for the lanthanum complex, which formed in approximately 70% yield.



Na₃(La)(trinitrotriolate)₂ **38.** A solution of 100 mg (0.233 mmol) of trinitrotriol **18** was placed in a 25 ml volumetric flask. 0.75 ml (3.1 mmol) of .97M NaOH in methanol was added. Methanol was added to make 25 ml of solution (9.3

mM). The solution changed from an orange to a deep purple as the NaOH was added. A 30 mg (85 μ mol) sample of $\text{LaCl}_3 \cdot 6\text{H}_2\text{O}$ was dissolved in 2 ml methanol. A 20 ml Schlenk flask was charged with 18.4 ml (171 μ mol) of 9.3 mM trinitrotriolate solution. To this Schlenk flask was added the LaCl_3 solution. Upon addition the purple solution turned back to yellow. The methanol was removed and a red brown solid was isolated. Yield was not determined. $^1\text{H-NMR}$ δ (ppm) 7.58 (d, 1H), 7.75 (dd, 1H), 7.87 (d, 1H)

3.3. IR

The solid complexes appeared to have some stability in air so IR samples of La 1:1 **28**, Gd 2:1 **32**, Yb 1:1 **30**, and trisodium triolate **27** were prepared in air by grinding 1-5 mg of sample with approximately 100 mg KBr and pelletized in a manual press. The FTIR spectra were obtained on a Nicolet IR/42. Data were collected from 4000 cm^{-1} to 400 cm^{-1} at room temp and under N_2 . Selected spectra are presented in the appendix (Figures A1-A4).

3.4. NMR Studies

Sodium triolate **27** was titrated with lanthanum chloride in D_2O . A 1.0 M NaOD solution was prepared by placing 46 mg sodium metal in a 2 ml volumetric flask and adding cold D_2O to the 2 ml mark. Triol **3** (2.3 mg, 0.0078 μ mol) was placed in a NMR tube and 0.5 ml D_2O , 24.9 μL NaOD (1.0M, 0.030 μ mol, 3.8 eq) was added. A stock solution was made by dissolving 8.5 mg (0.024 μ mol) $\text{LaCl}_3 \cdot 6\text{H}_2\text{O}$ in D_2O to make 1 ml of solution. LaCl_3 solution was added in 2 μL

aliquots until 20 μL had been added, after which the precipitate present interfered with the lock signal. NMR spectra were taken after each addition.

3.5. SQUID Measurements

Magnetic susceptibility measurements in the temperature range from 1.8 K to 300 K and -200 G to 50 kG were performed on a MPMS Quantum Design SQUID magnetometer. Powdered or microcrystalline samples were weighed and placed in a "baggie" (a piece of DOW Ziploc bag heat-sealed to form a small bag ca. 1.5 x 5 cm). The baggie was evacuated and refilled with argon three times, and then evacuated and heat sealed. The excess baggie was trimmed off with standard scissors and then reweighed. The sample weight was found by subtracting the weight of an equal size piece (typically 4.5 x 0.5 cm) of ziplog bag from the sealed and trimmed baggie weight. The sample was placed in a normal drinking straw (origin not known), and its position was fixed securely with white thread. The sample straw was attached to the SQUID sample rod and centered according to the length of the sample from the top of the rod. It was then placed in the air-lock on the instrument. The air was evacuated and replaced with helium 3 times before the sample was lowered into the experimental chamber.

The sample was positioned in a 200 G external magnetic field according to the centering scheme built into the machine. Magnetic susceptibility measurements were conducted using a general sequence consisting of field dependence measurements from -200 G to 50,000 G at 1.8 K followed by temperature dependence measurements from 1.8 K to 300 K at 200 G. The data

collected were extracted into data files consisting of temperatures in K, external field strength in gauss, induced magnetic moments in emu, and their standard deviations. The molecular formulas used are assumed to be the same as found in the X-ray structures. The Yb 1:1 complex **33** was assumed to have the same structure as the Gd 1:1 complex **29** (based on thermogravimetric analysis and expected structural similarities). The data were plotted and fitted using Mathcad 3.0 by Mathsoft Inc., 1991.

3.6. X-ray crystallography

Crystal data for Na₃Gd(triolate)₂ **32**, Na₃Yb(triolate)₂ **33**, La₂(triolate)₂ **28**, and Gd₂(triolate)₂ **29** are given in Table A1-A4. Atomic positional and isotropic thermal parameters can be found in Table A5-A12. Intensity data were collected on either a Rigaku AFC6S diffractometer or a Siemens/Nicolet NICOLET diffractometer, with graphite monochromated Mo K α radiation. Structures were solved using SHELXLS³⁹ and refined by full-matrix least-squares procedures on F² using SHELXL97⁴⁰. Data collection and analysis were done with the direct assistance of Dr. D. Ward.

La₂(triolate)₂•6DMSO 28: A colorless needle of C₄₈H₆₀N₂O₁₂S₆La₂ having the approximate dimensions 0.1 x 0.1 x 0.2 mm was mounted on a glass fiber with a drop of EXXON "paratone-N" oil. The fiber was placed in a stream of N₂ at -100 °C. A total of 5186 reflections ($\pm h$, $\pm k$, $\pm l$) were collected in a range 0.94° < θ < 22.45° with 5186 unique reflections used in the refinement of 631 variables. Final R = 0.0526, wR² = 0.1434

Gd₂(triolate)₂•4DMSO 29: A colorless rod of C₄₄H₄₈N₂O₁₀S₄Gd₂ having the approximate dimensions 0.1 x 0.1 x 0.4 mm was mounted on a glass fiber with a drop of oil. The fiber was placed in a stream of N₂ at –100 °C. A total of 5421 reflections ($\pm h$, $\pm k$, $\pm l$) were collected in a range $4^\circ < 2\theta < 50^\circ$ with 5324 having $I_o > 0.1 \sigma(I_o)$ being used in the refinement of 377 variables. Final R = 0.0318, $wR^2 = 0.0727$.

Na₃Gd(triolate)₂•2H₂O•6CH₃OH 32: A colorless needle of C₄₂H₅₂N₂O₁₄GdNa₃ with the approximate dimensions 0.1 x 0.1 x 0.6 mm was mounted on a glass fiber with a drop of oil. The fiber was placed in a stream of N₂ at –100 °C. A total of 2927 reflections ($\pm h$, $\pm k$, $\pm l$) were collected in a range $4^\circ < 2\theta < 40^\circ$ with 2107 having $I_o > 0.05 \sigma(I_o)$ being used in the refinement of 322 variables. Final R = 0.0526, $wR^2 = 0.1268$. It should be noted that the data crystal was lost midway into the third shell of data collection (40–45 degrees 2θ). Because of this (and to maintain a constant resolution in all directions in reciprocal space) data with 2θ greater than 40 degrees either was never collected or was discarded. This resulted in a data set containing only half the expected number of reflections for this crystal. This lack of data forced us to highly constrain our model. Some of the constraints include forcing the phenyl rings to have all the same C-C distances, the same C-C-C bond angles, and all carbons lying on the same plane. The hydrogen atoms were also fixed on their corresponding carbons at idealized positions.

Na₃Yb(triolate)₂•2H₂O•5CH₃OH 33: A colorless needle of C₄₁H₄₈N₂O₁₃YbNa₃ with the approximate dimensions 0.07 x 0.1 x 0.2 mm was

mounted on a glass fiber with a drop of oil. The fiber was placed in a stream of N_2 at $-100\text{ }^{\circ}\text{C}$. A total of 4162 reflections ($\pm h, \pm k, \pm l$) were collected in a range $2.45^{\circ} < \theta < 22.37^{\circ}$ with 3832 having $I_o > 0.05 \sigma(I_o)$ being used in the refinement of 358 variables. Final $R = 0.0655$, $wR^2 = 0.1541$

As with **32** the data set for **33** was also incomplete as coincidentally the data crystal was lost at about the same point as in the Gd 2:1 crystal **32**. The lack of data forced us to refine all atoms as isotropic except for Yb1, Na3, and Na4. The structure was also highly constrained using the same constraints as were used for the Gd 2:1 **32** complex.

APPENDIX

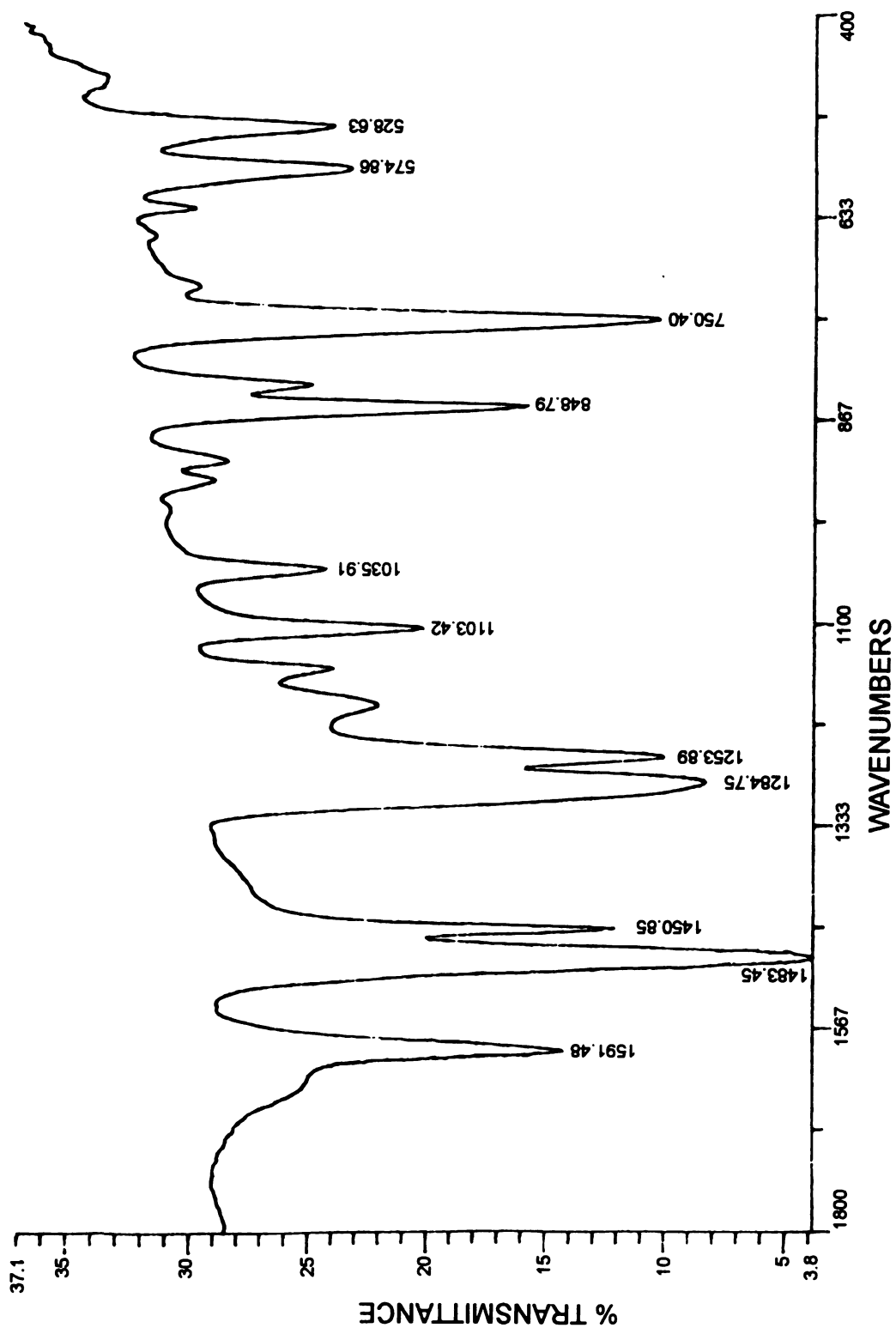


Figure A.1: FTIR spectrum of $\text{Yb}_2(\text{triolate})_2 \cdot 4\text{DMSO}$ 30 (KBr pellet).

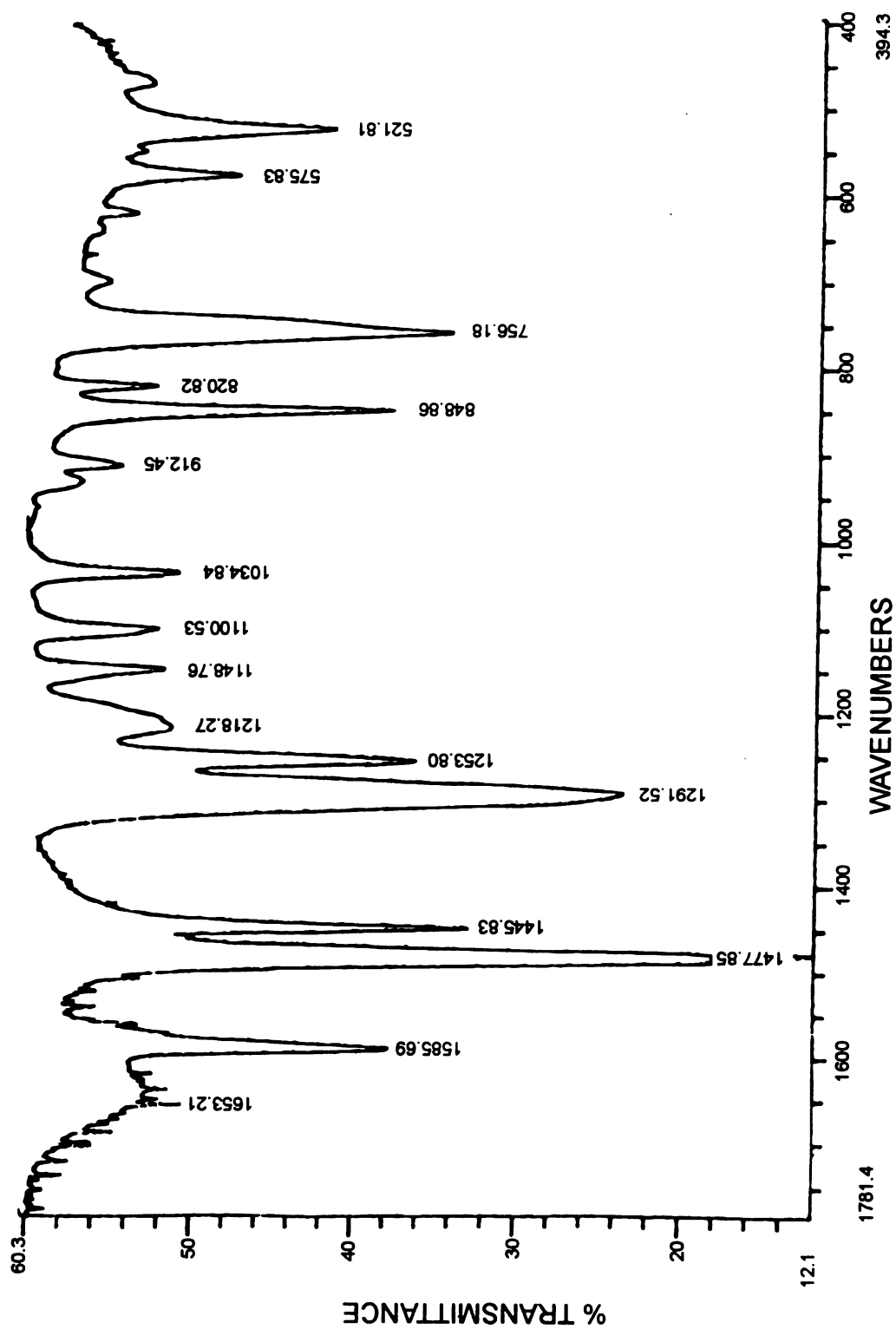


Figure A.2: FTIR spectrum of $\text{Na}_3\text{Gd}(\text{triolate})_2 \cdot 2\text{H}_2\text{O} \cdot 6\text{CH}_3\text{OH}$ 32 (KBr pellet).

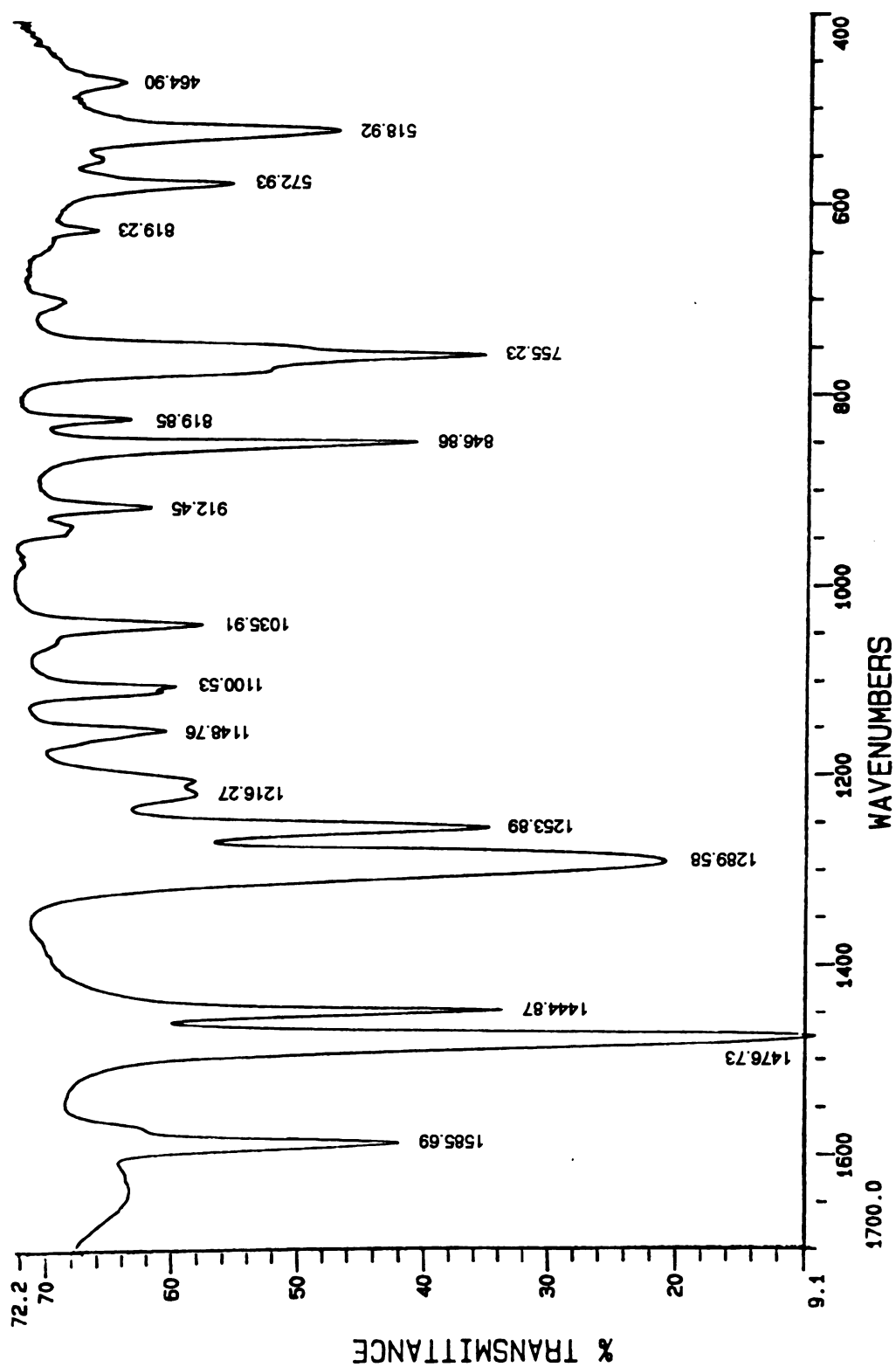


Figure A.3: FTIR spectrum of $\text{Na}_3\text{La}(\text{triolate})_2 \cdot 2\text{H}_2\text{O} \cdot 6\text{CH}_3\text{OH}$ 31 (KBr pellet).

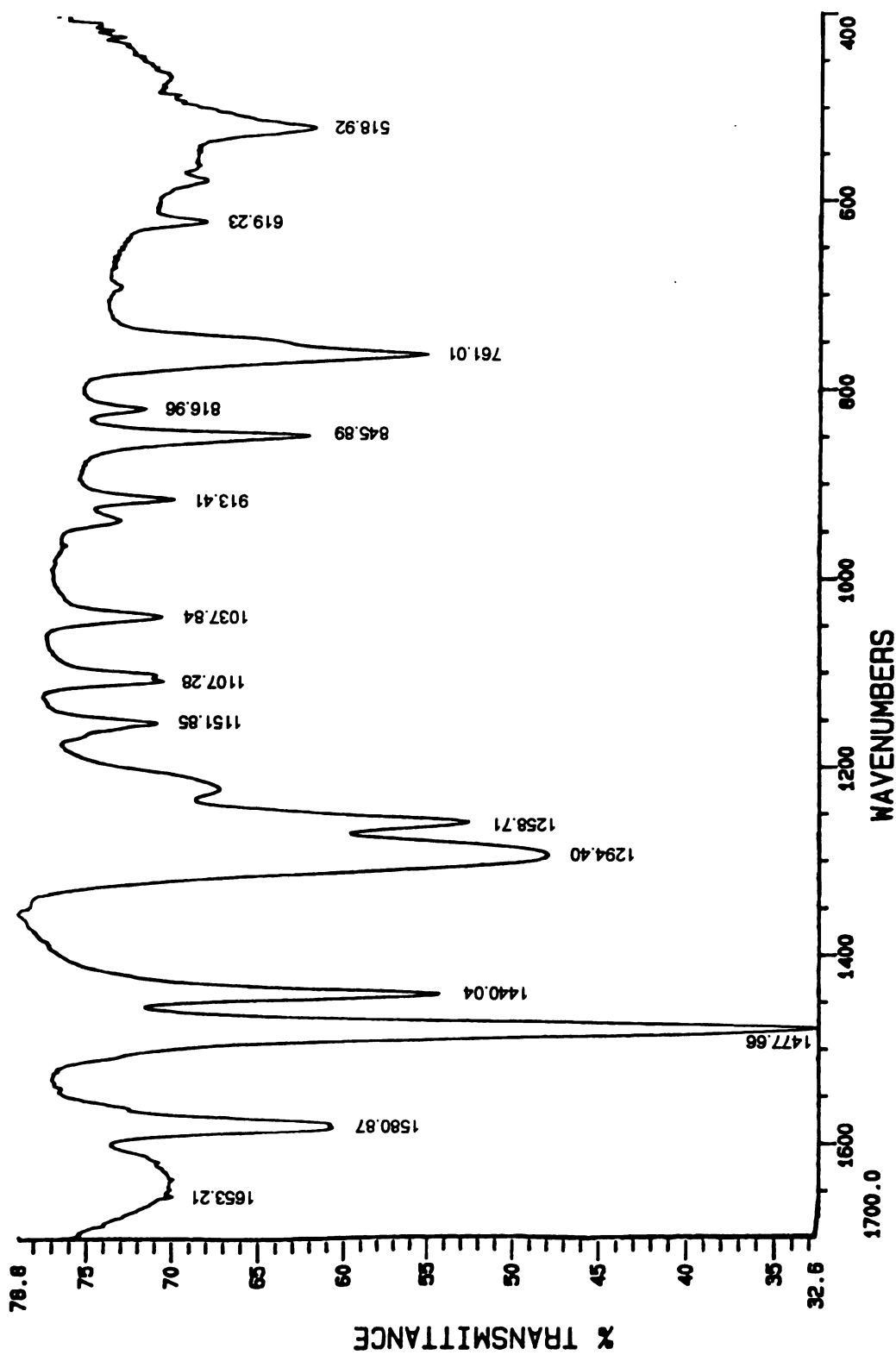


Figure A.4: FTIR spectrum of trisodium triolate 27 (KBr pellet).

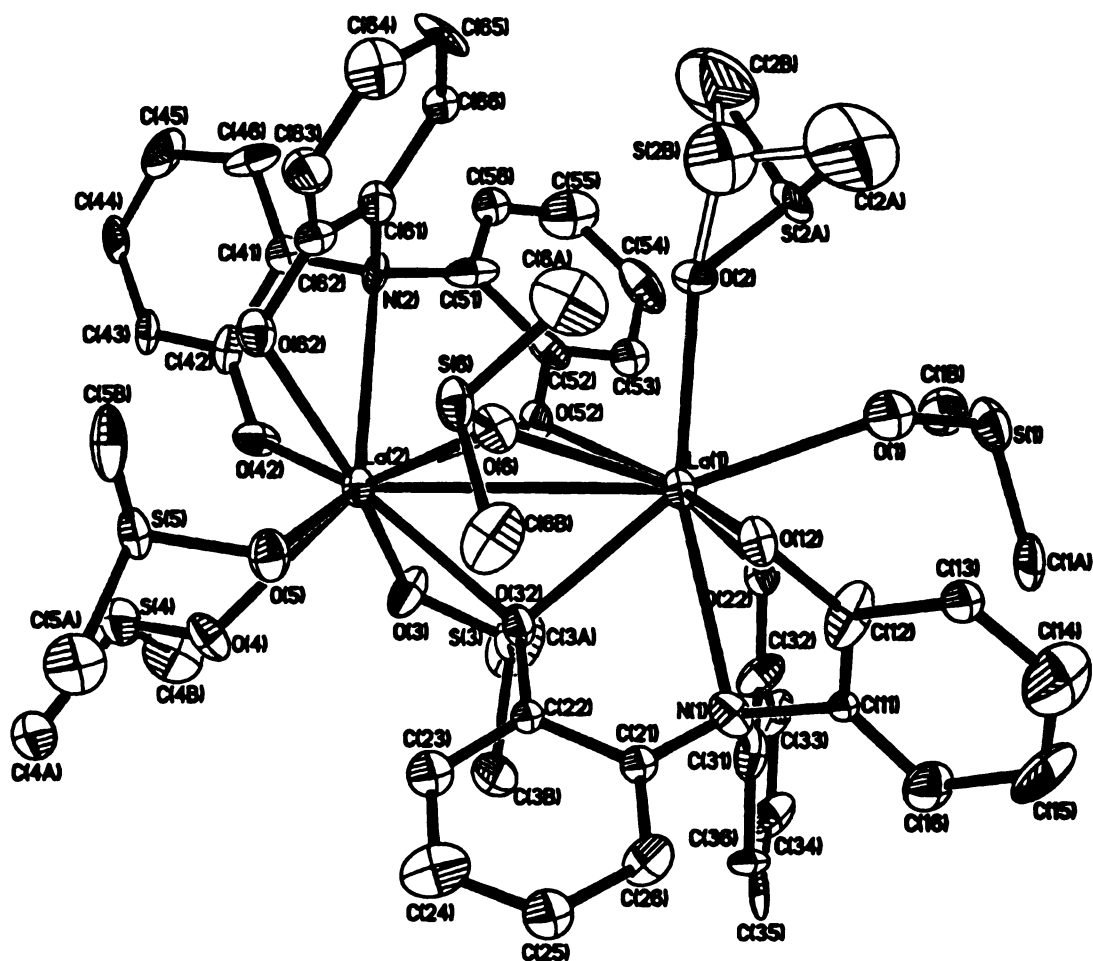


Figure A.5: Drawing of $\text{La}_2(\text{triolate})_2 \cdot 6\text{DMSO}$ 28 showing thermal ellipsoids and atom labeling scheme. Hydrogens are omitted.

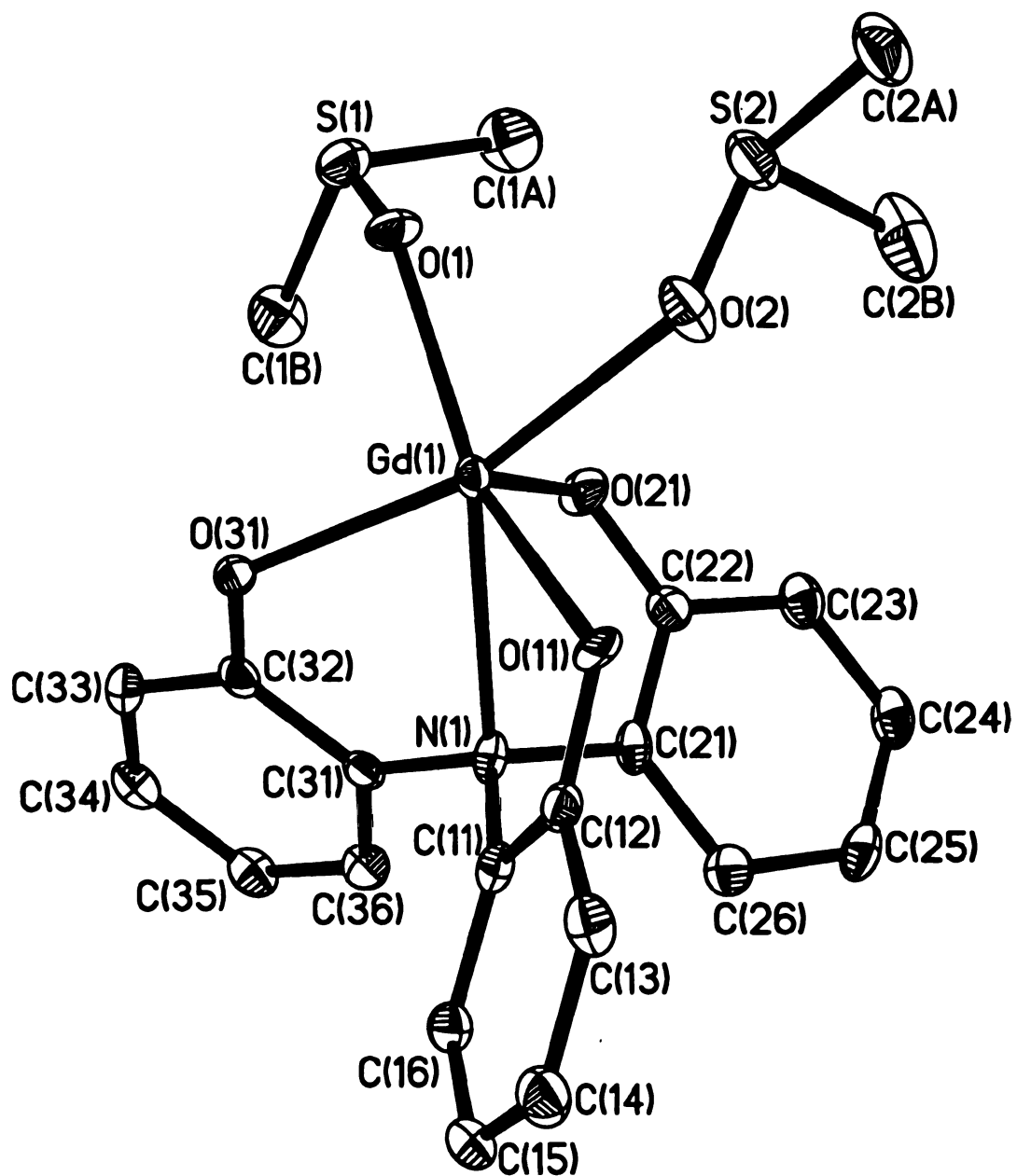


Figure A.6: Drawing of $\text{Gd}_2(\text{triolate})_2 \cdot 4\text{DMSO}$ **29** showing thermal ellipsoids and atom labeling scheme. Hydrogens are omitted.

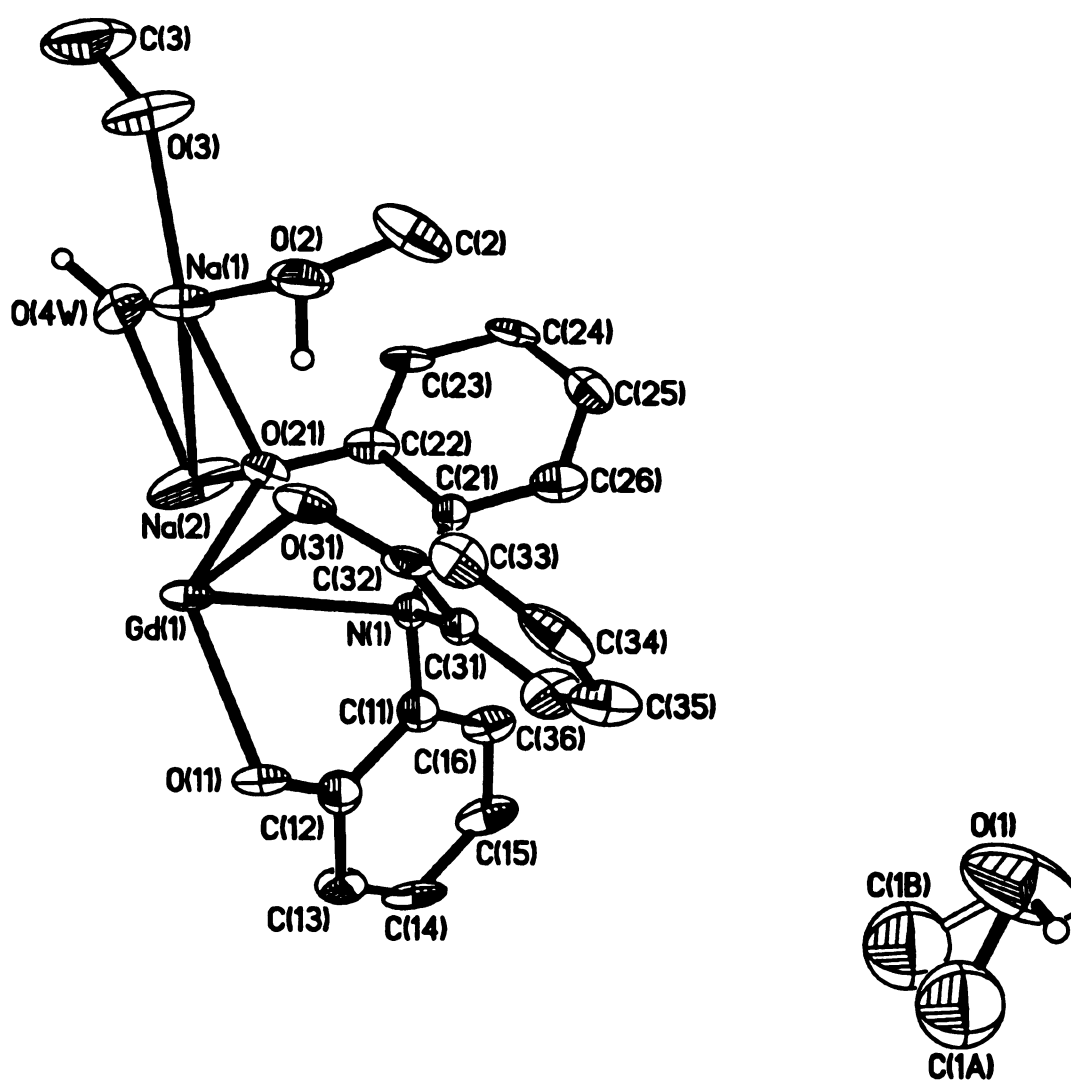


Figure A.7: Drawing of $\text{Na}_3\text{Gd}(\text{triolate})_2 \cdot 2\text{H}_2\text{O} \cdot 6\text{CH}_3\text{OH}$ **32** showing thermal ellipsoids and atom labeling scheme. Hydrogens are omitted.

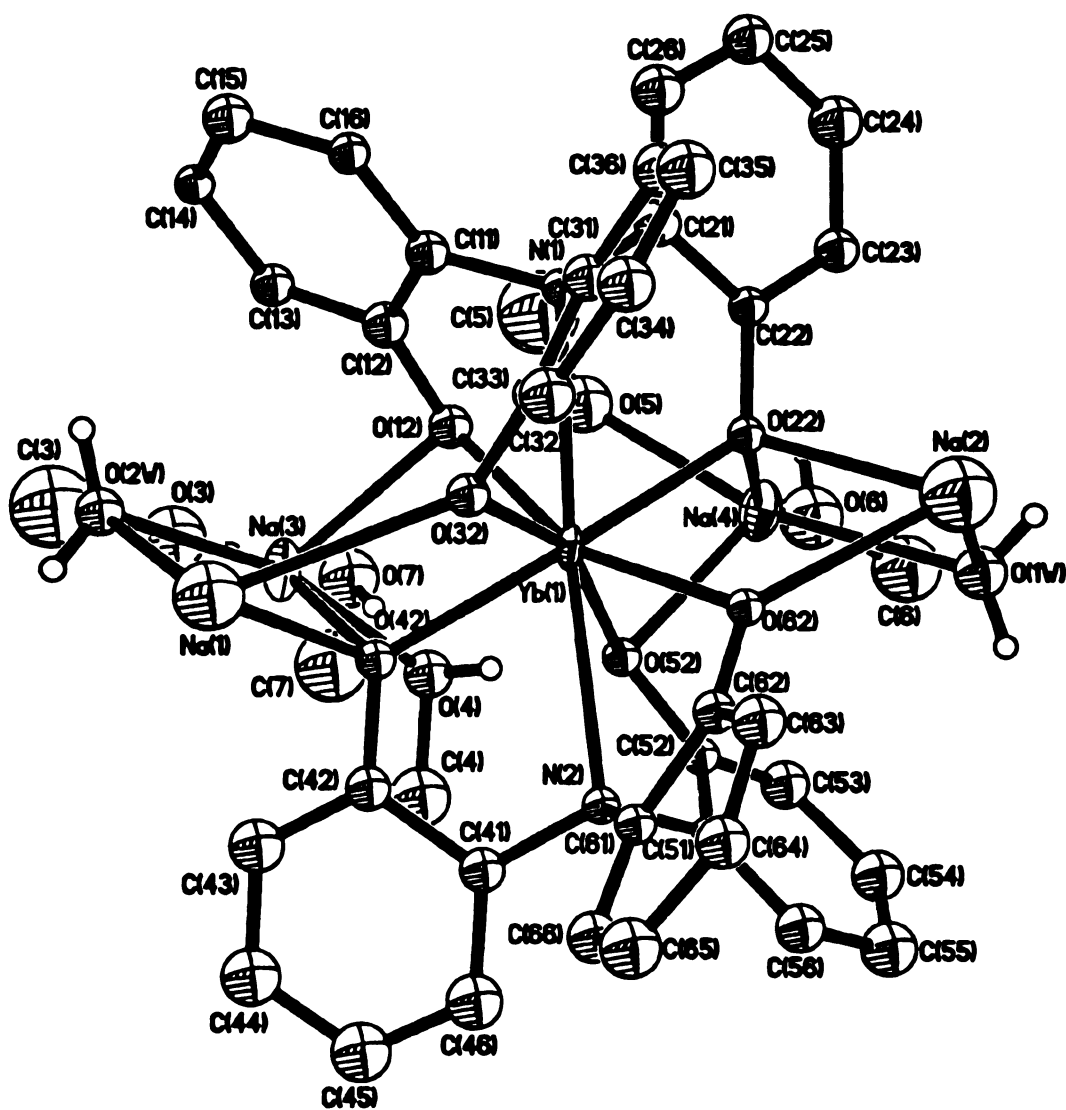


Figure A.8: Drawing of $\text{Na}_3\text{Yb}(\text{triolate})_2 \cdot 2\text{H}_2\text{O} \cdot 5\text{CH}_3\text{OH}$ 33 showing thermal ellipsoids and atom labeling scheme. Hydrogens are omitted.

Table A.1: Crystallographic data for La₂(triolate)₂•6DMSO 28

Empirical formula	C ₄₈ H ₆₀ La ₂ N ₂ O ₁₂ S ₆
Formula weight	1327.16
Temperature	173(3) K
Wavelength	0.70926 Å
Crystal system	triclinic
Space group	P-1 (# 2)
Unit cell dimensions	a = 13.401(5) Å b = 21.930(12) Å c = 10.193(5) Å α = 100.28(4) deg. β = 112.28(3) deg. γ = 83.37(4) deg.
Volume	2724(2) Å ³
Z	2
Density (calculated)	1.618 Mg/m ³
Absorption coefficient	1.837 mm ⁻¹
F(000)	1336
Crystal size	0.1 x 0.1 x 0.2 mm
Theta range for data collection	0.94 to 22.45 deg.
Index ranges	0 ≤ h ≤ 12, -23 ≤ k ≤ 23, -10 ≤ l ≤ 10
Reflections collected / unique	5186 / 5186 [R(int) = 0.0000]
Completeness to theta = 22.45	72.80%
Refinement method	Full-matrix least-squares on F ²
Data / restraints / parameters	5186 / 144 / 631
Goodness-of-fit on F ²	1.178
Final R indices [I > 2σ(I)]	R ₁ = 0.0526, wR ₂ = 0.1434
R indices (all data)	R ₁ = 0.1101, wR ₂ = 0.1854
Largest diff. peak and hole	0.980 and -1.034 eÅ ⁻³

Table A.2: Crystallographic data for Gd₂(triolate)₂•4DMSO 29

Empirical formula	C ₂₂ H ₂₄ GdNO ₅ S ₂
Formula weight	603.79
Temperature	293(2) K
Wavelength	0.71069 Å
Crystal system	triclinic
Space group	P-1 (# 2)
Unit cell dimensions	a = 10.314(2) Å b = 10.360(2) Å c = 11.404(2) Å α = 80.37(2) deg. β = 76.33(2) deg. γ = 77.66(2) deg.
Volume	1147.9(4) Å ³
Z	2
Density (calculated)	1.747 Mg/m ³
Absorption coefficient	3.104 mm ⁻¹
F(000)	598
Crystal size	0.1 x 0.1 x 0.4 mm
Theta range for data collection	2.57 to 27.61 deg.
Index ranges	-6 ≤ h ≤ 13, -13 ≤ k ≤ 13, -14 ≤ l ≤ 14
Reflections collected / unique	5421 / 5324 [R(int) = 0.0427]
Completeness to theta =27.61	99.6%
Refinement method	Full-matrix least-squares on F ²
Data / restraints / parameters	5324 / 0 / 377
Goodness-of-fit on F ²	1.090
Final R indices [I>2σ(I)]	R ₁ = 0.0318, wR ₂ = 0.0727
R indices (all data)	R ₁ = 0.0388, wR ₂ = 0.0762
Extinction coefficient	0.0034(4)
Largest diff. peak and hole	1.247 and -1.730 e. Å ⁻³

Table A.3: Crystallographic data for Na₃Gd(triolate)₂•2H₂O•6CH₃OH **32**

Empirical formula	C ₂₁ H ₂₆ Gd _{0.50} NNa _{1.50} O ₇
Formula weight	517.54
Temperature	173(3) K
Wavelength	0.71069 Å
Crystal system	monoclinic
Space group	C2/c (# 15)
Unit cell dimensions	a = 19.50(4) Å b = 15.313(11) Å c = 15.266(11) Å α = 90 deg. β = 90.71(12) deg. γ = 90 deg.
Volume	4559(10) Å ³
Z	8
Density (calculated)	1.508 Mg/m ³
Absorption coefficient	1.549 mm ⁻¹
F(000)	2108
Crystal size	0.1 x 0.1 x 0.6 mm
Theta range for data collection	2.66 to 19.97 deg.
Index ranges	0 ≤ h ≤ 18, 0 ≤ k ≤ 14, -14 ≤ l ≤ 14
Reflections collected / unique	2184 / 2107 [R(int) = 0.0549]
Completeness to theta = 19.97	99.80%
Refinement method	Full-matrix least-squares on F ²
Data / restraints / parameters	2107 / 9 / 322
Goodness-of-fit on F ²	1.123
Final R indices [I > 2σ(I)]	R ₁ = 0.0526, wR ₂ = 0.1268
R indices (all data)	R ₁ = 0.0698, wR ₂ = 0.1517
Largest diff. peak and hole	1.547 and -2.630 e. Å ⁻³

Table A.4: Crystallographic data for Na₃Yb(triolate)₂•2H₂O•5CH₃OH **33**

Empirical formula	C ₄₁ H ₄₈ N ₂ Na ₃ O ₁₃ Yb
Formula weight	1018.82
Temperature	213(5) K
Wavelength	0.71069 Å
Crystal system	triclinic
Space group	P-1 (# 2)
Unit cell dimensions	a = 12.450 Å b = 13.179 Å c = 15.262 Å α = 111.35 deg. β = 90.16 deg. γ = 110.68 deg.
Volume	2157.1 Å ³
Z	2
Density (calculated)	1.569 Mg/m ³
Absorption coefficient	2.263 mm ⁻¹
F(000)	1030
Crystal size	0.07 x 0.1 x 0.2 mm
Theta range for data collection	2.45 to 22.54 deg.
Index ranges	-2 ≤ h ≤ 7, -14 ≤ k ≤ 13, -16 ≤ l ≤ 16
Reflections collected / unique	4162 / 3832 [R(int) = 0.0542]
Completeness to theta = 22.54	67.30%
Refinement method	Full-matrix least-squares on F ²
Data / restraints / parameters	3832 / 1519 / 358
Goodness-of-fit on F ²	1.115
Final R indices [I>2σ(I)]	R1 = 0.0655, wR2 = 0.1541
R indices (all data)	R1 = 0.1040, wR2 = 0.1906
Largest diff. peak and hole	2.216 and -1.649 e. Å ⁻³

Table A.5: Atomic coordinates ($\times 10^4$), equivalent isotropic displacement parameters ($\text{\AA}^2 \times 10^3$), and occupancies for $\text{La}_2(\text{triolate})_2 \cdot 6\text{DMSO}$ **28**

Atom	x	y	z	U(eq)	Occ.
La(1)	2217(1)	3188(1)	8073(1)	21(1)	1
La(2)	1651(1)	1580(1)	5471(1)	19(1)	1
S(1)	2260(5)	5002(2)	9054(6)	36(2)	1
S(2A)	-302(6)	4222(3)	7223(9)	32(3)	0.74(2)
S(2B)	-850(30)	3792(15)	7310(30)	73(13)	0.26(2)
S(3)	3744(4)	2407(2)	5179(6)	30(1)	1
S(4)	2621(5)	174(3)	3629(6)	38(2)	1
S(5)	1460(4)	186(2)	6562(5)	26(1)	1
S(6)	801(4)	1853(2)	8697(6)	26(1)	1
O(1)	1914(11)	4373(6)	8982(14)	36(4)	1
O(2)	227(11)	3564(7)	7264(17)	48(4)	1
O(3)	3001(11)	1867(6)	4489(14)	35(4)	1
O(4)	2844(11)	570(6)	5062(13)	29(3)	1
O(5)	1924(11)	830(6)	7260(13)	29(3)	1
O(6)	1197(10)	2173(6)	7782(13)	25(3)	1
O(12)	2610(11)	3197(6)	10562(13)	25(3)	1
O(22)	3406(11)	3732(5)	7534(13)	23(3)	1
O(32)	3243(10)	2157(5)	7624(13)	22(3)	1
O(42)	1109(11)	1252(6)	2940(14)	26(3)	1
O(52)	1414(10)	2720(5)	5567(13)	20(3)	1
O(62)	-83(11)	1185(6)	5061(13)	26(3)	1
N(1)	4405(13)	3058(7)	9774(16)	24(4)	1
N(2)	-356(12)	2108(7)	3549(15)	17(4)	1
C(1B)	2205(17)	5074(10)	7310(20)	38(6)	1
C(1A)	3675(17)	5013(9)	9910(20)	36(6)	1
C(2B)	-1520(30)	4090(15)	5760(40)	105(12)	1
C(2A)	-730(30)	4338(17)	8670(30)	103(12)	1
C(3B)	5028(16)	2048(10)	6110(20)	41(6)	1
C(3A)	4020(20)	2605(12)	3730(20)	57(8)	1
C(4B)	3246(19)	497(11)	2670(20)	48(7)	1
C(4A)	3535(17)	-487(10)	4030(20)	43(6)	1
C(5B)	511(19)	109(9)	7290(20)	39(6)	1
C(5A)	2460(18)	-330(11)	7510(20)	48(7)	1
C(6B)	1964(18)	1755(11)	10260(20)	42(6)	1
C(6A)	72(19)	2468(11)	9450(20)	48(7)	1
C(11)	4406(15)	3526(8)	11040(19)	13(5)	1
C(12)	3454(19)	3554(11)	11330(20)	36(6)	1
C(13)	3409(16)	3981(8)	12530(20)	22(5)	1
C(14)	4270(20)	4333(13)	13380(30)	60(8)	1

Table A.5: continued

Atom	x	y	z	U(eq)	Occ.
C(15)	5221(19)	4279(12)	13120(20)	48(7)	1
C(16)	5282(18)	3817(10)	11940(20)	32(6)	1
C(21)	4596(15)	2437(9)	9990(20)	19(5)	1
C(22)	4008(15)	1983(8)	8783(19)	16(5)	1
C(23)	4268(16)	1345(9)	8940(20)	29(5)	1
C(24)	4994(18)	1158(13)	10160(20)	44(6)	1
C(25)	5504(17)	1611(9)	11360(20)	32(6)	1
C(26)	5312(16)	2237(10)	11240(20)	30(5)	1
C(31)	5035(18)	3272(9)	9060(20)	26(5)	1
C(32)	4444(17)	3586(10)	7900(20)	29(5)	1
C(33)	5059(18)	3778(10)	7170(20)	34(6)	1
C(34)	6149(18)	3614(11)	7530(20)	37(6)	1
C(35)	6690(20)	3297(9)	8640(20)	31(6)	1
C(36)	6120(15)	3127(9)	9400(20)	19(5)	1
C(41)	-701(16)	1705(9)	2210(20)	25(5)	1
C(42)	156(18)	1263(8)	1970(20)	20(5)	1
C(43)	-160(18)	901(9)	610(20)	24(5)	1
C(44)	-1188(18)	893(9)	-360(20)	29(5)	1
C(45)	-1993(19)	1278(10)	-70(20)	39(6)	1
C(46)	-1738(16)	1701(11)	1220(20)	33(6)	1
C(51)	-138(16)	2726(10)	3410(20)	30(6)	1
C(52)	789(17)	3015(9)	4460(20)	25(5)	1
C(53)	1087(16)	3559(9)	4300(20)	25(5)	1
C(54)	424(19)	3885(10)	3160(20)	41(6)	1
C(55)	-490(20)	3600(12)	2130(20)	45(7)	1
C(56)	-753(17)	3063(9)	2310(20)	25(5)	1
C(61)	-1064(16)	2099(9)	4320(20)	25(5)	1
C(62)	-867(15)	1622(9)	5105(19)	20(5)	1
C(63)	-1512(17)	1561(10)	5870(20)	37(6)	1
C(64)	-2302(19)	2031(11)	5910(30)	47(7)	1
C(65)	-2510(17)	2534(10)	5150(20)	37(6)	1
C(66)	-1889(15)	2573(9)	4360(20)	20(5)	1
H(1B1)	1467	5075	6656	50	1
H(1B2)	2608	4731	6983	50	1
H(1B3)	2510	5455	7346	50	1
H(1A1)	3874	4976	10906	47	1
H(1A2)	3916	5396	9836	47	1
H(1A3)	4007	4671	9465	47	1
H(2B1)	-1200(110)	3800(110)	5190(160)	136	0.74(2)
H(2B2)	-1660(150)	4510(40)	5600(200)	136	0.74(2)
H(2B3)	-1870(120)	3930(130)	6300(150)	136	0.74(2)

Table A.5: continued

Atom	x	y	z	U(eq)	Occ.
H(2B4)	-1100(300)	3900(300)	5200(300)	136	0.26(2)
H(2B5)	-1400(500)	4520(40)	6140(190)	136	0.26(2)
H(2B6)	-2220(140)	3900(300)	5500(400)	136	0.26(2)
H(2A1)	-30(80)	4250(140)	9370(110)	133	0.74(2)
H(2A2)	-1240(180)	4020(100)	8290(190)	133	0.74(2)
H(2A3)	-1000(200)	4760(50)	8600(200)	133	0.74(2)
H(2A4)	0(200)	4200(200)	9300(300)	133	0.26(2)
H(2A5)	-1300(400)	4300(200)	9000(500)	133	0.26(2)
H(2A6)	-800(600)	4710(40)	8200(200)	133	0.26(2)
H(3B1)	5014	1916	6956	53	1
H(3B2)	5578	2340	6388	53	1
H(3B3)	5182	1695	5501	53	1
H(3A1)	3392	2805	3107	74	1
H(3A2)	4226	2235	3207	74	1
H(3A3)	4606	2882	4107	74	1
H(4B1)	2845	869	2353	62	1
H(4B2)	3259	203	1860	62	1
H(4B3)	3971	594	3290	62	1
H(4A1)	3317	-725	4575	56	1
H(4A2)	4251	-353	4583	56	1
H(4A3)	3526	-740	3157	56	1
H(5B1)	-122	368	6877	50	1
H(5B2)	808	232	8307	50	1
H(5B3)	321	-316	7081	50	1
H(5A1)	3078	-347	7248	72	1
H(5A2)	2183	-736	7293	72	1
H(5A3)	2665	-189	8524	72	1
H(6B1)	2449	1438	10023	54	1
H(6B2)	1747	1635	10974	54	1
H(6B3)	2320	2138	10636	54	1
H(6A1)	-598	2572	8720	63	1
H(6A2)	498	2826	9835	63	1
H(6A3)	-72	2332	10206	63	1
H(13)	2787	4023	12745	10(40)	1
H(14)	4210	4616	14143	80(90)	1
H(15)	5794	4527	13682	20(50)	1
H(16)	5936	3725	11803	0(40)	1
H(23)	3926	1045	8181	0(40)	1
H(24)	5158	737	10221	180(190)	1
H(25)	5967	1487	12221	10(40)	1
H(26)	5670	2528	12014	10(50)	1

Table A.5: continued

Atom	x	y	z	U(eq)	Occ.
H(33)	4717	4017	6434	70(90)	1
H(34)	6518	3723	7004	50(70)	1
H(35)	7421	3196	8894	60(90)	1
H(36)	6486	2907	10159	0(40)	1
H(43)	367	652	357	50(70)	1
H(44)	-1351	626	-1220	0(40)	1
H(45)	-2700	1260	-728	50(70)	1
H(46)	-2271	1975	1402	10(50)	1
H(53)	1733	3722	4952	80(80)	1
H(54)	590	4277	3106	0(40)	1
H(55)	-900	3784	1320	500(600)	1
H(56)	-1394	2900	1651	30(70)	1
H(63)	-1420	1219	6336	60(80)	1
H(64)	-2706	2011	6468	40(60)	1
H(65)	-3056	2834	5168	30(60)	1
H(66)	-2001	2906	3865	90(90)	1

U(eq) is defined as one third of the trace of the orthogonalized U_{ij} tensor.

Table A.6: Anisotropic displacement parameters ($\text{\AA}^2 \times 10^3$) for
La₂(triolate)₂•6DMSO 28

Atom	U11	U22	U33	U23	U13	U12
La(1)	24(1)	16(1)	22(1)	1(1)	9(1)	-2(1)
La(2)	24(1)	17(1)	18(1)	0(1)	10(1)	-3(1)
S(1)	45(4)	19(3)	50(4)	2(3)	27(3)	-1(3)
S(2A)	31(5)	9(5)	62(6)	12(4)	23(4)	6(3)
S(3)	34(3)	23(3)	35(3)	-4(3)	19(3)	-6(3)
S(4)	39(4)	29(3)	37(4)	-6(3)	10(3)	0(3)
S(5)	38(3)	13(3)	27(3)	1(2)	12(3)	-2(2)
S(6)	36(3)	17(3)	32(3)	1(2)	19(3)	-6(3)
O(2)	17(8)	41(10)	70(12)	-21(8)	11(8)	1(7)
O(3)	35(9)	39(9)	32(9)	-12(7)	17(7)	-20(7)
O(4)	43(9)	21(8)	24(8)	4(6)	16(7)	10(7)
O(5)	39(9)	24(8)	22(8)	1(6)	11(7)	-3(7)
O(6)	34(9)	25(8)	24(8)	7(6)	19(7)	0(7)
O(12)	34(9)	17(8)	27(8)	1(6)	15(7)	-1(7)
O(22)	29(10)	15(8)	30(8)	6(6)	15(7)	-8(7)
O(32)	30(8)	15(8)	19(8)	2(6)	6(7)	0(6)
O(42)	21(9)	37(9)	16(8)	-1(6)	7(8)	7(7)
O(52)	27(8)	13(7)	20(8)	8(6)	6(7)	-1(6)
O(62)	33(9)	23(8)	25(8)	-1(6)	16(7)	-2(7)
N(1)	34(11)	26(10)	17(9)	5(8)	17(8)	5(8)
N(2)	24(10)	16(10)	13(9)	-6(7)	11(8)	-10(8)
C(1B)	35(14)	39(14)	46(15)	2(11)	20(12)	-7(11)
C(1A)	51(15)	14(12)	39(14)	-5(10)	14(12)	-8(11)
C(2B)	100(30)	80(30)	100(30)	20(20)	0(20)	40(20)
C(2A)	110(30)	150(30)	70(20)	-10(20)	70(20)	10(20)
C(3B)	32(14)	36(14)	53(16)	-2(12)	19(12)	4(11)
C(3A)	73(19)	73(19)	45(16)	16(14)	32(14)	-37(16)
C(4B)	57(17)	60(17)	35(14)	5(12)	30(13)	6(14)
C(4A)	38(15)	31(14)	49(16)	-4(11)	9(12)	1(11)
C(5B)	73(18)	16(12)	37(14)	5(10)	27(13)	-15(12)
C(6B)	54(16)	53(16)	28(13)	12(11)	20(12)	-21(13)
C(6A)	60(17)	68(18)	40(15)	19(13)	41(14)	5(14)
C(12)	53(16)	52(16)	11(12)	-12(11)	21(12)	-24(14)
C(14)	60(20)	90(20)	25(15)	-11(15)	21(14)	-14(16)
C(15)	35(16)	80(20)	17(13)	-5(13)	0(12)	-24(15)
C(16)	34(15)	40(14)	19(13)	2(11)	6(11)	-3(11)
C(24)	35(15)	65(19)	38(15)	18(13)	14(12)	-6(13)
C(26)	33(14)	33(14)	23(13)	14(11)	4(11)	-11(11)
C(31)	41(16)	20(12)	22(13)	-2(10)	15(12)	-13(11)

Table A.6: continued

Atom	U11	U22	U33	U23	U13	U12
C(32)	23(15)	40(14)	27(13)	6(11)	7(12)	-16(12)
C(33)	36(16)	31(14)	29(14)	-2(11)	5(12)	-13(12)
C(34)	30(16)	63(17)	16(13)	-10(12)	10(12)	-15(13)
C(35)	53(18)	14(12)	24(14)	-15(10)	19(13)	-6(11)
C(36)	10(13)	27(12)	16(11)	5(10)	3(10)	3(10)
C(42)	38(15)	16(12)	9(12)	3(9)	9(11)	-10(10)
C(43)	34(15)	11(11)	24(13)	-1(10)	8(12)	-8(11)
C(44)	42(16)	15(12)	22(13)	-9(10)	7(13)	-4(11)
C(45)	35(16)	45(16)	23(14)	-14(12)	0(13)	-17(13)
C(46)	13(13)	52(16)	36(15)	21(12)	4(11)	-4(12)
C(51)	14(13)	56(16)	20(12)	8(11)	6(11)	5(11)
C(52)	32(14)	22(12)	28(13)	8(10)	21(12)	10(11)
C(54)	63(18)	21(14)	55(17)	18(12)	36(15)	14(13)
C(55)	42(16)	69(19)	23(13)	9(13)	10(13)	-1(14)
C(61)	30(13)	20(12)	28(12)	0(10)	14(11)	-4(10)
C(62)	17(12)	31(13)	10(11)	-6(10)	7(10)	-2(11)
C(63)	29(14)	30(14)	60(16)	6(12)	28(13)	-3(11)
C(65)	35(14)	32(14)	57(16)	5(12)	37(13)	19(12)

The anisotropic displacement factor exponent takes the form:

$$-2 \pi^2 [h^2 a^{*2} U11 + \dots + 2 h k a^* b^* U12]$$

Table A.7: Atomic coordinates ($\times 10^4$), equivalent isotropic displacement parameters ($\text{\AA}^2 \times 10^3$), and occupancies for $\text{Gd}_2(\text{triolate})_2 \cdot 4\text{DMSO}$ **29**

Atom	x	y	z	U(eq)	Occ.
Gd(1)	666(1)	-247(1)	1488(1)	13(1)	1
S(1)	2683(1)	2277(1)	-96(1)	23(1)	1
S(2)	894(1)	1879(1)	3543(1)	26(1)	1
O(1)	1432(3)	1784(3)	671(3)	19(1)	1
O(2)	178(4)	887(4)	3221(3)	26(1)	1
O(11)	-718(3)	-1494(3)	2769(3)	17(1)	1
O(21)	2868(3)	-960(3)	1761(3)	19(1)	1
O(31)	1108(3)	-813(3)	-485(3)	14(1)	1
N(1)	1529(4)	-2811(4)	1366(3)	15(1)	1
C(1A)	3799(6)	2103(6)	931(6)	33(1)	1
C(1B)	3591(6)	947(6)	-943(5)	29(1)	1
C(2A)	-304(7)	2694(6)	4697(5)	34(1)	1
C(2B)	2032(7)	882(8)	4442(6)	42(2)	1
C(11)	308(4)	-3389(4)	1740(4)	16(1)	1
C(12)	-785(4)	-2679(4)	2523(4)	16(1)	1
C(13)	-1924(5)	-3279(5)	3014(4)	20(1)	1
C(14)	-1996(5)	-4504(5)	2708(4)	23(1)	1
C(15)	-937(5)	-5162(5)	1898(4)	22(1)	1
C(16)	217(5)	-4605(4)	1415(4)	18(1)	1
C(21)	2374(4)	-3150(4)	2276(4)	15(1)	1
C(22)	3051(4)	-2145(4)	2407(4)	17(1)	1
C(23)	3879(5)	-2464(5)	3278(4)	21(1)	1
C(24)	3997(5)	-3689(5)	3995(4)	23(1)	1
C(25)	3305(5)	-4643(5)	3868(4)	22(1)	1
C(26)	2490(5)	-4377(5)	2997(4)	19(1)	1
C(31)	2295(4)	-2943(4)	133(4)	14(1)	1
C(32)	2035(4)	-1884(4)	-772(4)	15(1)	1
C(33)	2779(5)	-1993(5)	-1964(4)	19(1)	1
C(34)	3740(5)	-3115(5)	-2238(4)	20(1)	1
C(35)	3998(5)	-4163(5)	-1340(4)	20(1)	1
C(36)	3278(4)	-4066(4)	-160(4)	18(1)	1
H(1B3)	4540(80)	900(70)	-1380(70)	50(20)	1
H(1A1)	3940(60)	1150(70)	1420(60)	41(17)	1
H(1A2)	3390(60)	2740(60)	1490(50)	26(14)	1
H(1B1)	3210(40)	710(40)	-1570(40)	2(10)	1
H(1B2)	3650(50)	160(50)	-330(50)	14(12)	1
H(1A3)	4620(60)	2300(60)	480(60)	34(16)	1
H(2B1)	2680(80)	340(80)	3900(70)	60(20)	1
H(2A3)	-530(80)	2050(80)	5310(70)	60(20)	1

Table A.7: continued

Atom	x	y	z	U(eq)	Occ.
H(2A1)	160(80)	3210(80)	5010(70)	60(20)	1
H(2A2)	-1030(80)	3140(70)	4350(70)	60(20)	1
H(2B2)	2460(80)	1490(80)	4740(70)	60(20)	1
H(2B3)	1600(80)	380(70)	5100(70)	50(20)	1
H(13)	-2710(50)	-2820(50)	3530(50)	21(13)	1
H(14)	-2850(50)	-4830(50)	3070(50)	19(13)	1
H(15)	-980(50)	-5970(60)	1680(50)	23(14)	1
H(16)	970(60)	-5070(50)	850(50)	24(14)	1
H(23)	4320(60)	-1840(60)	3410(50)	28(15)	1
H(24)	4550(50)	-3850(50)	4580(50)	22(13)	1
H(25)	3430(60)	-5440(60)	4340(50)	26(14)	1
H(26)	2030(60)	-4980(60)	2880(50)	26(14)	1
H(33)	2640(50)	-1280(50)	-2560(40)	12(11)	1
H(34)	4330(50)	-3150(50)	-3110(50)	21(13)	1
H(35)	4700(50)	-5030(50)	-1530(50)	19(13)	1
H(36)	3440(50)	-4780(50)	520(40)	10(11)	1

U(eq) is defined as one third of the trace of the orthogonalized U_{ij} tensor.

Table A.8: Anisotropic displacement parameters ($\text{\AA}^2 \times 10^3$) for
Gd₂(triolate)₂•4DMSO 29

Atom	U11	U22	U33	U23	U13	U12
Gd(1)	14(1)	14(1)	11(1)	-2(1)	-6(1)	-1(1)
S(1)	26(1)	19(1)	24(1)	2(1)	-6(1)	-7(1)
S(2)	32(1)	29(1)	19(1)	-10(1)	-3(1)	-9(1)
O(1)	22(2)	13(1)	22(2)	1(1)	-3(1)	-7(1)
O(2)	28(2)	36(2)	20(2)	-12(1)	-4(1)	-12(2)
O(11)	21(2)	14(1)	12(1)	4(1)	2(1)	-10(1)
O(21)	18(2)	16(2)	24(2)	3(1)	-12(1)	-1(1)
O(31)	16(1)	10(1)	16(1)	-3(1)	-6(1)	3(1)
N(1)	14(2)	19(2)	10(2)	1(1)	-4(1)	0(1)
C(1A)	26(3)	36(3)	40(3)	-4(3)	-13(2)	-10(2)
C(1B)	26(3)	35(3)	25(3)	-7(2)	2(2)	-6(2)
C(2A)	44(3)	34(3)	22(3)	-15(2)	-8(2)	10(3)
C(2B)	36(3)	59(4)	32(3)	-20(3)	-14(3)	6(3)
C(11)	17(2)	18(2)	12(2)	2(2)	-5(2)	-3(2)
C(12)	18(2)	18(2)	11(2)	2(2)	-4(2)	-8(2)
C(13)	21(2)	26(2)	15(2)	-5(2)	-3(2)	-5(2)
C(14)	24(2)	29(2)	18(2)	-2(2)	-6(2)	-11(2)
C(15)	29(2)	23(2)	20(2)	-3(2)	-10(2)	-11(2)
C(16)	19(2)	18(2)	17(2)	-1(2)	-7(2)	-3(2)
C(21)	11(2)	22(2)	12(2)	-2(2)	-5(2)	1(2)
C(22)	17(2)	16(2)	18(2)	-4(2)	-7(2)	0(2)
C(23)	20(2)	25(2)	19(2)	-3(2)	-9(2)	-1(2)
C(24)	21(2)	29(2)	18(2)	-3(2)	-11(2)	4(2)
C(25)	23(2)	23(2)	15(2)	3(2)	-7(2)	2(2)
C(26)	16(2)	20(2)	19(2)	-2(2)	-5(2)	-1(2)
C(31)	16(2)	12(2)	15(2)	-5(2)	-6(2)	-1(2)
C(32)	15(2)	16(2)	18(2)	-4(2)	-8(2)	-3(2)
C(33)	21(2)	22(2)	13(2)	0(2)	-6(2)	-4(2)
C(34)	20(2)	23(2)	19(2)	-9(2)	-3(2)	-5(2)
C(35)	16(2)	21(2)	24(2)	-9(2)	-5(2)	1(2)
C(36)	16(2)	17(2)	20(2)	-3(2)	-6(2)	1(2)

The anisotropic displacement factor exponent takes the form:
 $-2 \pi^2 [h^2 a^{*2} U11 + \dots + 2 h k a^* b^* U12]$

Table A.9: Atomic coordinates ($\times 10^4$), equivalent isotropic displacement parameters ($\text{\AA}^2 \times 10^3$), and occupancies for $\text{Na}_3\text{Gd}(\text{triolate})_2 \cdot 2\text{H}_2\text{O} \cdot 6\text{CH}_3\text{OH}$ **32**

Atom	x	y	z	U(eq)	Occ.
Gd(1)	0	528(1)	2500	23(1)	1
Na(1)	11(3)	2170(3)	753(3)	38(1)	1
Na(2)	0	0	0	76(3)	1
O(1)	4453(8)	737(8)	6744(9)	100(5)	1
C(1A)	4150(30)	-90(40)	6990(40)	84(19)	0.57(9)
C(1B)	3880(40)	230(50)	6730(40)	80(20)	0.43(9)
O(2)	732(5)	2961(5)	1883(6)	44(2)	1
C(2)	1407(8)	3181(10)	1618(10)	56(4)	1
O(3)	-151(6)	3561(6)	213(7)	71(3)	1
C(3)	-524(11)	3852(11)	-523(14)	92(7)	1
O(4W)	-435(7)	1427(6)	-525(7)	36(3)	1
O(11)	406(4)	-643(4)	3359(4)	21(2)	1
O(21)	475(4)	787(5)	1106(5)	26(2)	1
O(31)	717(4)	1681(5)	3056(5)	30(2)	1
N(1)	1345(4)	237(6)	2400(6)	18(2)	1
C(11)	1384(6)	-715(8)	2418(7)	25(3)	1
C(12)	873(6)	-1118(8)	2928(8)	29(3)	1
C(13)	869(7)	-2037(7)	2956(9)	33(3)	1
C(14)	1345(7)	-2507(8)	2524(8)	36(3)	1
C(15)	1836(7)	-2110(8)	2010(8)	36(3)	1
C(16)	1851(6)	-1207(8)	1966(7)	29(3)	1
C(21)	1627(5)	657(7)	1637(7)	20(3)	1
C(22)	1147(7)	907(7)	971(7)	24(3)	1
C(23)	1402(6)	1284(7)	225(7)	24(3)	1
C(24)	2090(7)	1459(8)	143(8)	33(3)	1
C(25)	2547(7)	1259(8)	792(9)	35(3)	1
C(26)	2313(7)	851(8)	1542(8)	31(3)	1
C(31)	1612(5)	635(7)	3224(7)	18(3)	1
C(32)	1302(6)	1408(8)	3487(7)	26(3)	1
C(33)	1574(7)	1866(9)	4188(9)	33(3)	1
C(34)	2107(9)	1496(12)	4644(13)	48(6)	1
C(35)	2405(9)	728(10)	4422(9)	41(4)	1
C(36)	2147(8)	307(10)	3692(10)	36(4)	1
H(1O)	4540(70)	840(100)	7370(110)	70(50)	1
H(1A1)	4470(80)	-540(110)	7350(100)	10(40)	0.57(9)
H(1A2)	3970(90)	-60(110)	7360(120)	0(60)	0.57(9)
H(1A3)	4080(120)	-420(150)	6300(160)	70(70)	0.57(9)
H(2O)	729	2510	2304	100(60)	1
H(2A)	1668	2657	1533	300(200)	1

Table A.9: continued

Atom	x	y	z	U(eq)	Occ.
H(2B)	1624	3532	2063	50(40)	1
H(2C)	1385	3504	1079	100(70)	1
H(3A)	-400(100)	4380(110)	-810(130)	230(90)	1
H(3B)	-1000(80)	3980(160)	-480(110)	230(90)	1
H(3C)	-560(120)	3490(120)	-1030(110)	230(90)	1
H(4WA)	-170(50)	1360(80)	-770(70)	0(40)	1
H(4WB)	-810(80)	1660(110)	-1000(110)	90(60)	1
H(13)	535	-2325	3276	0(20)	1
H(14)	1342	-3113	2573	20(30)	1
H(15)	2150	-2443	1701	10(30)	1
H(16)	2179	-931	1627	20(30)	1
H(23)	1103	1424	-234	30(30)	1
H(24)	2246	1720	-367	30(30)	1
H(25)	3009	1393	733	0(20)	1
H(26)	2623	707	1987	50(40)	1
H(33)	1360(70)	2490(110)	4240(90)	70(50)	1
H(34)	2220(50)	1750(70)	4980(70)	0(40)	1
H(35)	2790(60)	470(80)	4650(80)	30(40)	1
H(36)	2370(50)	-110(70)	3530(60)	0(30)	1

U(eq) is defined as one third of the trace of the orthogonalized U_{ij} tensor.

Table A.10: Anisotropic displacement parameters ($\text{\AA}^2 \times 10^3$) for
 $\text{Na}_3\text{Gd}(\text{triolate})_2 \cdot 2\text{H}_2\text{O} \cdot 6\text{CH}_3\text{OH}$ **32**

Atom	U11	U22	U33	U23	U13	U12
Gd(1)	41(1)	11(1)	17(1)	0	3(1)	0
Na(1)	61(3)	19(3)	34(3)	6(2)	1(2)	0(2)
Na(2)	143(9)	19(4)	63(6)	-9(4)	-69(6)	3(5)
O(1)	158(14)	71(9)	70(9)	-6(7)	9(9)	-56(9)
O(2)	56(6)	24(5)	52(6)	13(5)	0(5)	-6(5)
C(2)	79(12)	38(9)	51(10)	-7(8)	19(9)	-31(9)
O(3)	123(10)	34(6)	57(7)	18(6)	-15(7)	15(6)
C(3)	126(17)	55(12)	93(15)	43(11)	-33(14)	-5(11)
O(4W)	46(7)	29(6)	33(6)	-10(5)	6(6)	14(5)
O(11)	45(5)	13(4)	6(4)	-2(3)	6(4)	5(4)
O(21)	33(5)	23(5)	22(4)	2(4)	0(4)	-8(4)
O(31)	50(6)	13(4)	25(5)	-5(4)	11(4)	-6(4)
C(13)	41(8)	8(7)	49(9)	5(6)	7(7)	4(7)
C(14)	67(10)	6(7)	36(8)	7(6)	0(8)	9(7)
C(15)	63(10)	19(8)	25(8)	-3(6)	3(7)	18(7)
C(16)	46(8)	30(9)	10(6)	3(6)	6(6)	9(7)
C(22)	47(9)	12(6)	12(7)	-7(6)	-2(6)	-3(6)
C(23)	46(9)	13(7)	12(7)	3(5)	0(6)	-4(6)
C(24)	47(10)	18(7)	33(8)	11(6)	3(8)	-11(6)
C(25)	32(8)	31(8)	40(9)	-1(7)	10(7)	-8(7)
C(26)	49(9)	25(7)	20(7)	0(6)	0(7)	2(6)
C(32)	34(8)	28(8)	16(7)	13(6)	2(6)	-6(6)
C(33)	42(9)	26(8)	32(8)	-10(7)	1(7)	-6(7)
C(34)	69(14)	45(14)	31(10)	-10(10)	10(10)	-40(12)
C(35)	67(11)	26(10)	30(9)	2(8)	1(8)	-8(9)
C(36)	52(9)	11(8)	46(10)	-10(7)	-3(8)	3(8)

The anisotropic displacement factor exponent takes the form:
 $-2 \pi^2 [h^2 a^{*2} U_{11} + \dots + 2 h k a^* b^* U_{12}]$

Table A.11: Atomic coordinates ($\times 10^4$), equivalent isotropic displacement parameters ($\text{\AA}^2 \times 10^3$), and occupancies for $\text{Na}_3\text{Yb}(\text{triolate})_2 \cdot 2\text{H}_2\text{O} \cdot 5\text{CH}_3\text{OH}$ **33**

Atom	x	y	z	U(eq)	Occ.
Yb(1)	632(1)	496(1)	2641(1)	16(1)	1
Na(1)	0	0	0	48(3)	1
Na(2)	0	0	5000	59(3)	1
Na(3)	2548(6)	2165(5)	1449(4)	29(2)	1
Na(4)	2593(6)	2146(5)	4907(4)	29(2)	1
O(1W)	2023(6)	833(7)	5790(5)	32(3)	1
O(2W)	1335(10)	1948(5)	130(3)	24(3)	1
O(3)	4029(9)	3789(9)	1398(6)	52(4)	1
C(3)	4210(20)	4404(19)	792(15)	84(8)	1
O(4)	4025(7)	2118(7)	2494(6)	28(3)	1
C(4)	4733(16)	1476(14)	2142(12)	45(5)	1
O(5)	2943(9)	3688(8)	4381(5)	41(3)	1
C(5)	3210(30)	4899(13)	4635(18)	89(8)	1
O(6)	4235(12)	3308(11)	5994(8)	53(4)	1
C(6)	4807(19)	3106(18)	6673(13)	61(6)	1
O(7)	5566(11)	4381(5)	2969(8)	49(3)	1
C(7)	6675(17)	4360(20)	2822(16)	75(7)	1
N(1)	-760(9)	1680(7)	3102(5)	14(3)	1
C(11)	-431(7)	2439(10)	2573(9)	19(4)	1
C(12)	768(10)	2863(10)	2494(9)	22(4)	1
O(12)	1475(7)	2424(7)	2753(6)	20(2)	1
C(13)	1190(11)	3738(9)	2113(8)	20(4)	1
C(14)	377(10)	4067(8)	1746(9)	16(3)	1
C(15)	-788(10)	3576(9)	1761(10)	24(4)	1
C(16)	-1189(9)	2759(10)	2186(9)	17(3)	1
C(21)	-498(10)	2392(9)	4120(6)	22(4)	1
C(22)	210(12)	2126(9)	4658(8)	16(3)	1
O(22)	612(9)	1276(6)	4241(5)	15(2)	1
C(23)	494(10)	2802(9)	5647(6)	21(4)	1
C(24)	117(14)	3700(11)	6070(6)	30(4)	1
C(25)	-566(14)	3970(10)	5533(8)	26(4)	1
C(26)	-847(13)	3321(12)	4563(9)	26(4)	1
C(31)	-1910(9)	745(9)	2781(7)	20(4)	1
C(32)	-1960(9)	-242(9)	1949(8)	15(3)	1
O(32)	-1001(7)	-238(7)	1556(6)	17(2)	1
C(33)	-3038(7)	-1167(9)	1554(9)	26(4)	1
C(34)	-3994(10)	-1157(9)	2005(9)	25(4)	1
C(35)	-3928(12)	-213(10)	2836(9)	28(4)	1
C(36)	-2895(13)	737(9)	3206(9)	26(4)	1

Table A.11: continued

Atom	x	y	z	U(eq)	Occ.
N(2)	1272(8)	-1335(8)	1990(6)	14(3)	1
C(41)	1985(10)	-1226(9)	1250(8)	21(4)	1
C(42)	1938(11)	-402(10)	857(9)	20(4)	1
O(42)	1297(8)	241(7)	1205(6)	16(2)	1
C(43)	2627(10)	-263(10)	162(8)	30(4)	1
C(44)	3300(11)	-923(10)	-181(10)	36(4)	1
C(45)	3365(13)	-1686(11)	224(10)	39(5)	1
C(46)	2684(15)	-1863(14)	911(10)	33(4)	1
C(51)	1976(13)	-1205(6)	2817(7)	11(3)	1
C(52)	2668(13)	-21(8)	3395(8)	15(3)	1
O(52)	2507(9)	870(6)	3266(6)	16(2)	1
C(53)	3447(13)	164(9)	4152(8)	27(4)	1
C(54)	3465(14)	-781(10)	4345(8)	30(4)	1
C(55)	2751(14)	-1925(9)	3777(9)	33(4)	1
C(56)	2000(14)	-2130(8)	3000(9)	25(4)	1
C(61)	159(9)	-2328(8)	1682(7)	15(3)	1
C(62)	-696(12)	-2114(8)	2252(7)	17(3)	1
O(62)	-452(8)	-1085(6)	2986(5)	14(2)	1
C(63)	-1771(9)	-3034(7)	2007(9)	25(4)	1
C(64)	-2001(9)	-4096(9)	1237(9)	23(4)	1
C(65)	-1191(12)	-4237(10)	652(10)	31(4)	1
C(66)	-92(13)	-3359(11)	897(9)	24(4)	1
H(1O)	4540(70)	840(100)	7370(110)	70(50)	1
H(1A1)	4470(80)	-540(110)	7350(100)	10(40)	0.57(9)
H(1A2)	3970(90)	-60(110)	7360(120)	0(60)	0.57(9)
H(1A3)	4080(120)	-420(150)	6300(160)	70(70)	0.57(9)
H(2O)	729	2510	2304	100(60)	1
H(2A)	1668	2657	1533	300(200)	1
H(2B)	1624	3532	2063	50(40)	1
H(2C)	1385	3504	1079	100(70)	1
H(3A)	-400(100)	4380(110)	-810(130)	230(90)	1
H(3B)	-1000(80)	3980(160)	-480(110)	230(90)	1
H(3C)	-560(120)	3490(120)	-1030(110)	230(90)	1
H(4WA)	-170(50)	1360(80)	-770(70)	0(40)	1
H(4WB)	-810(80)	1660(110)	-1000(110)	90(60)	1
H(13)	535	-2325	3276	0(20)	1
H(14)	1342	-3113	2573	20(30)	1
H(15)	2150	-2443	1701	10(30)	1
H(16)	2179	-931	1627	20(30)	1
H(23)	1103	1424	-234	30(30)	1
H(24)	2246	1720	-367	30(30)	1

Table A.11: continued

Atom	x	y	z	U(eq)	Occ.
H(25)	3009	1393	733	0(20)	1
H(26)	2623	707	1987	50(40)	1
H(33)	1360(70)	2490(110)	4240(90)	70(50)	1
H(34)	2220(50)	1750(70)	4980(70)	0(40)	1
H(35)	2790(60)	470(80)	4650(80)	30(40)	1
H(36)	2370(50)	-110(70)	3530(60)	0(30)	1

U(eq) is defined as one third of the trace of the orthogonalized U_{ij} tensor.

Table A.12: Anisotropic displacement parameters ($\text{\AA}^2 \times 10^3$) for
 $\text{Na}_3\text{Yb}(\text{triolate})_2 \cdot 2\text{H}_2\text{O} \cdot 5\text{CH}_3\text{OH}$ 33

Atom	U11	U22	U33	U23	U13	U12
Yb(1)	19(1)	21(1)	10(1)	11(1)	1(1)	7(1)
Na(3)	30(7)	34(3)	22(3)	17(3)	-1(3)	4(3)
Na(4)	25(7)	32(3)	27(3)	16(3)	-4(3)	3(3)

The anisotropic displacement factor exponent takes the form:
 $-2 \pi^2 [h^2 a^{*2} U_{11} + \dots + 2 h k a^* b^* U_{12}]$

LIST OF REFERENCES

LIST OF REFERENCES

1. B. Kahr, J. E. Jackson, D. L. Ward, S.-H. Jang, J. F. Blount, *Acta Crystallogr. Sect. B struct. Sci.*, **1992**, *48*, 324.
2. S.-H. Jang, *Ph.D Dissertation*, MSU **1993**.
3. S. J. Stoudt, *Ph.D Dissertation*, MSU **1995**.
4. Karl A. Gscheidner, LeRoy Eyring, Handbook on the Physics and Chemistry of Rare Earths, Volume 4 Non-Metallic Compounds II, 1979.
5. For simplicity 2,2',2''-nitrilotriphenol or (tris(2-hydroxyphenyl)amine) are referred to as triol and the trianion of 2,2',2''-nitrilotriphenol is then triolate.
6. C.L. Frye, G.A. Vincent, G.L. Hauschildt, *J. Am. Chem. Soc.* **1966**, *88*, 2727.
7. E. Müller, H. B. Bürgi, *Helv. Chim. Acta.* **1987**, *70*, 499.
8. E. Müller, H. B. Bürgi, *Helv. Chim. Acta.* **1987**, *70*, 511.
9. M. A. Paz-Sandoval, C. Fernandez-Vincent, G. Uribe, R. Contreras, *Polyhedron*, **1988**, *7*, 679.
10. E. Müller, H. B. Bürgi, *Helv. Chim. Acta.* **1987**, *70*, 520.
11. E. Müller, H. B. Bürgi, *Helv. Chim. Acta.* **1987**, *70*, 1063.
12. J. G. Verkade, *Coordin. Chem. Rev.* **1994**, *137*, 233.

13. P. Livant, J. Northcott, T. R. Webb, *J. Organomet. Chem.*, **2001**, *20*, 133.
14. M. D. Ravenscroft, R. M. G., *J. Organomet. Chem.*, **1986**, *312*, 33.
15. C. Soulie, P. Bassoul, J. Simon, *J. Chem. Soc., Chem. Commun.* **1993**, *2*, 114.
16. C. Soulie, *Tetrahedron*, **2001**, *57*, 1035.
17. C. Soulie, P. Bassoul, J. Simon, *New J. Chem.* **1993**, *17(12)*, 787.
18. E. Müller, H. B. Bürgi, *Acta Crystallogr. Sec. C: Cryst. Struct. Commun.* **1989**, *C45(9)*, 1400.
19. G. E. Freeman, K. N. Raymond, *Inorg. Chem.*, **1985**, *24*, 1410.
20. S. Liu L. Gelmini, S. J. Rettig, R. C. Thompson, C. Orvig, *J. Am. Chem. Soc.* **1992**, *114*, 6081.
21. A. Panagiotopoulos, T. F. Zafiropoulos, S. P. Perlepes, E. Bakalbassis, I. Masson-Ramade, O. Kahn, A. Terzis, C. P. Raptopoulos, *Inorg. Chem.*, **1995**, *34*, 4918-4920.
22. P. Guerriero, S. Tamburini, and P.A. Vigato, *Inorganica Chimica Acta*, **1991**, *189*, 19.
23. J. P. Costes, F. Dahan, A. Dupuis, S. Lagrave, J. P. Laurent, *Inorg. Chem.*, **1998**, *37*, 153.
24. R. Hedinger, M. Ghisletta, K. Hegetschweiler, E. Toth, A. E. Merbach, R. Sessoli, D. Gatteschi, V. Gramlich, *Inorg. Chem.*, **1998**, *37*, 6698.
25. S. Gauthier, J. M. J. Frechet, *Synth. Commun.* **1987**, *17*, 383.
26. S. J. Stoudt, P. Gopalan, A. Bakulin, B. Kahr, J. E. Jackson, *Inorg. Chem.*, **1996**, *35*, 6614.
27. S. Liu L. Gelmini, S. J. Rettig, R. C. Thompson, C. Orvig, *J. Am. Chem. Soc.* **1992**, *114*, 6081.

28. O. Kahn, Molecular Magnetism; VCH, 1993; chapter 2.
29. Y. Cui, F. Zheng, Y. Qian, J. Huang, *Inorganica Chimica Acta*, **2001**, 315, 220.
30. J. P. Costes, , A. Dupuis, J. P. Laurent, *Inorganica Chimica Acta*, **1998**, 268, 125.
31. Y. T. Li, C. W. Yan, N. Yi, *syn. Reactive. Inorg. Metal-Org. C.*, **1999**, 29, 1153.
32. X. H. Kong, C. W. Yan, Y. T. Li, D. Z. Liao, *Chinese J. Chem.*, **1999**, 17, 609.
33. W. Plass, G. Fries, *Z. Anorg. Allg. Chem.*, **1997**, 623, 1205.
34. C. W. Yan, Y. T. Li, *Polish J. Chem.*, **1999**, 73, 1237.
35. R. H. Zhang, H. M. Wang, D. Z. Liao, T. Y. Chen, H. G. Wang, X. K. Yao, *Chinese J. Chem.*, **1996**, 14, 506.
36. S. Y. Nui, J. Jin, X. L. Jin, Y. Cong, Z. Z. Yang, *Chin. Sci. Bull.*, **2000**, 45, 706.
37. A. Misiolek, R. Huang, B. Kahr, J. E. Jackson, *J. Chem. Soc., Chem. Commun.*, **1996**, 2119
38. A. Vogel, Textbook of Practical Organic Chemistry fourth edition; Longman Scientific & Technical, 1978; 696.
39. G. M. Sheldrick, SHELXLS97, University of Göttingen, Germany.
40. G. M. Sheldrick, SHELXL97, University of Göttingen, Germany.

MICHIGAN STATE LIBRARIES



3 1293 02316 3359